

# UC Davis

## UC Davis Previously Published Works

### Title

Naïve CD8 T cell IFN $\gamma$  responses to a vacuolar antigen are regulated by an inflammasome-independent NLRP3 pathway and *Toxoplasma gondii* ROP5

### Permalink

<https://escholarship.org/uc/item/3f5395ng>

### Journal

PLOS Pathogens, 16(8)

### ISSN

1553-7366

### Authors

Kongsomboonvech, Angel K  
Rodriguez, Felipe  
Diep, Anh L  
[et al.](#)

### Publication Date

2020

### DOI

10.1371/journal.ppat.1008327

Peer reviewed

## RESEARCH ARTICLE

# Naïve CD8 T cell IFN $\gamma$ responses to a vacuolar antigen are regulated by an inflammasome-independent NLRP3 pathway and *Toxoplasma gondii* ROP5

Angel K. Kongsomboonvech<sup>1</sup>, Felipe Rodriguez<sup>1</sup>, Anh L. Diep<sup>1</sup>, Brandon M. Justice<sup>1</sup>, Brayan E. Castellanos<sup>1</sup>, Ana Camejo<sup>2</sup>, Debanjan Mukhopadhyay<sup>3</sup>, Gregory A. Taylor<sup>4,5</sup>, Masahiro Yamamoto<sup>6</sup>, Jeroen P. J. Saeij<sup>2,3</sup>, Michael L. Reese<sup>7</sup>, Kirk D. C. Jensen<sup>1,8\*</sup>

**1** Department of Molecular and Cell Biology, University of California, Merced, Merced, California, United States of America, **2** Department of Biology, Massachusetts Institute of Technology, Cambridge, Massachusetts, United States of America, **3** Department of Pathology, Microbiology and Immunology, School of Veterinary Medicine, University of California, Davis, Davis, California, United States of America, **4** Departments of Medicine; Molecular Genetics and Microbiology; and Immunology; and Center for the Study of Aging and Human Development, Duke University Medical Center, Durham, North Carolina, United States of America, **5** Geriatric Research, Education, and Clinical Center, Durham VA Health Care System, Durham, North Carolina, United States of America, **6** Department of Immunoparasitology, Research Institute for Microbial Diseases, Osaka University, Osaka, Japan, **7** Department of Pharmacology, University of Texas, Southwestern Medical Center, Dallas, Texas, United States of America, **8** Health Sciences Research Institute, University of California, Merced, Merced, California, United States of America

\* [kjensen5@ucmerced.edu](mailto:kjensen5@ucmerced.edu)



## OPEN ACCESS

**Citation:** Kongsomboonvech AK, Rodriguez F, Diep AL, Justice BM, Castellanos BE, Camejo A, et al. (2020) Naïve CD8 T cell IFN $\gamma$  responses to a vacuolar antigen are regulated by an inflammasome-independent NLRP3 pathway and *Toxoplasma gondii* ROP5. *PLoS Pathog* 16(8): e1008327. <https://doi.org/10.1371/journal.ppat.1008327>

**Editor:** Eric Y. Denkers, University of New Mexico, UNITED STATES

**Received:** January 13, 2020

**Accepted:** July 5, 2020

**Published:** August 27, 2020

**Copyright:** © 2020 Kongsomboonvech et al. This is an open access article distributed under the terms of the [Creative Commons Attribution License](https://creativecommons.org/licenses/by/4.0/), which permits unrestricted use, distribution, and reproduction in any medium, provided the original author and source are credited.

**Data Availability Statement:** All relevant data are within the manuscript and its Supporting Information files.

**Funding:** The research was funded by the National Institutes of Health (NIH) 1R15AI131027, and a Hellman's Fellow award to K.D.C.J.; NIH R01AI080621 to J.P.J.S.; M.L.R. acknowledges funding from the Welch Foundation (I-1936-20170325) and National Science Foundation

## Abstract

Host resistance to *Toxoplasma gondii* relies on CD8 T cell IFN $\gamma$  responses, which if modulated by the host or parasite could influence chronic infection and parasite transmission between hosts. Since host-parasite interactions that govern this response are not fully elucidated, we investigated requirements for eliciting naïve CD8 T cell IFN $\gamma$  responses to a vacuolar resident antigen of *T. gondii*, TGD057. Naïve TGD057 antigen-specific CD8 T cells (T57) were isolated from transnuclear mice and responded to parasite-infected bone marrow-derived macrophages (BMDMs) in an antigen-dependent manner, first by producing IL-2 and then IFN $\gamma$ . T57 IFN $\gamma$  responses to TGD057 were independent of the parasite's protein export machinery ASP5 and MYR1. Instead, host immunity pathways downstream of the regulatory Immunity-Related GTPases (IRG), including partial dependence on Guanylate-Binding Proteins, are required. Multiple *T. gondii* ROP5 isoforms and allele types, including 'avirulent' ROP5A from clade A and D parasite strains, were able to suppress CD8 T cell IFN $\gamma$  responses to parasite-infected BMDMs. Phenotypic variance between clades B, C, D, F, and A strains suggest T57 IFN $\gamma$  differentiation occurs independently of parasite virulence or any known IRG-ROP5 interaction. Consistent with this, removal of ROP5 is not enough to elicit maximal CD8 T cell IFN $\gamma$  production to parasite-infected cells. Instead, macrophage expression of the pathogen sensors, NLRP3 and to a large extent NLRP1, were absolute requirements. Other members of the conventional inflammasome cascade are only partially required, as revealed by decreased but not abrogated T57 IFN $\gamma$  responses to

(MCB1553334); G.A.T. is funded by NIH grants AI135398 and AI145929; M.Y. is supported by the Research Program on Emerging and Re-emerging Infectious Diseases (JP19fk0108047), Japanese Initiative for Progress of Research on Infectious Diseases for Global Epidemic (JP19fm0208018), Strategic International Collaborative Research Program (19jm0210067h) from Agency for Medical Research and Development (AMED), Grant-in-Aid for Scientific Research on Innovative Areas (19H04809), for Scientific Research (B) (18KK0226 and 18H02642) and for Scientific Research (A) (19H00970) from Ministry of Education, Culture, Sports, Science and Technology of Japan; A.K.K. acknowledges a Distinguished Scholars Fellowship (School of Natural Sciences, UC Merced) and a President's Dissertation Year Fellowship (UC Merced); F.R. acknowledges an undergraduate fellowship from the University of California LEADS program and an NIH opportunity supplement accompanying NIH R15AI131027. The funders had no role in study design, data collection and analysis, decision to publish, or preparation of the manuscript.

**Competing interests:** The authors have declared that no competing interests exist.

parasite-infected ASC, caspase-1/11, and gasdermin D deficient cells. Moreover, IFN $\gamma$  production was only partially reduced in the absence of IL-12, IL-18 or IL-1R signaling. In summary, *T. gondii* effectors and host machinery that modulate parasitophorous vacuolar membranes, as well as NLR-dependent but inflammasome-independent pathways, determine the full commitment of CD8 T cells IFN $\gamma$  responses to a vacuolar antigen.

## Author summary

Parasites are excellent “students” of our immune system as they can deflect, antagonize and confuse the immune response making it difficult to vaccinate against these pathogens. In this report, we analyzed how a widespread parasite of mammals, *Toxoplasma gondii*, manipulates an immune cell needed for immunity to many intracellular pathogens, the CD8 T cell. Host pathways that govern CD8 T cell production of the immune protective cytokine, IFN $\gamma$ , were also explored. We hypothesized the secreted *T. gondii* virulence factor, ROP5, work to inhibit the MHC 1 antigen presentation pathway therefore making it difficult for CD8 T cells to see *T. gondii* antigens sequestered inside a parasitophorous vacuole. However, manipulation through *T. gondii* ROP5 does not fully explain how CD8 T cells commit to making IFN $\gamma$  in response to infection. Importantly, CD8 T cell IFN $\gamma$  responses to *T. gondii* require the pathogen sensor NLRP3 to be expressed in the infected cell. Other proteins associated with NLRP3 activation, including members of the conventional inflammasome activation cascade pathway, are only partially involved. Our results identify a novel pathway by which NLRP3 regulates T cell function and underscore the need for NLRP3-activating adjuvants in vaccines aimed at inducing CD8 T cell IFN $\gamma$  responses to parasites.

## Introduction

*Toxoplasma gondii* is a globally spread intracellular parasite that can infect nearly all warm-blooded vertebrates, including humans. Transmission between hosts occurs following ingestion of oocysts shed from the definitive feline host or predation of chronically infected animals harboring infectious ‘tissue cysts’. Immune modulation by the parasite during the first weeks of infection is therefore critical for *T. gondii* to establish latency and life cycle progression. The parasite accomplishes this by hiding and manipulating the immune system from within a specialized parasitophorous vacuole (PV) that is created during invasion. *T. gondii* releases ‘effector’ proteins from secretory organelles, including rhoptry proteins (ROP) that are injected into the host cytosol upon invasion, as well as dense granules (GRA) that are secreted into the lumen of the PV and aid its internal structure and formation. Many of these secreted ‘effectors’ manipulate host cell signaling pathways and shield the PV from host immune attack [1]. In mice, *T. gondii* uses several ROP and GRA proteins to antagonize the host’s Immunity-Related GTPases (IRGs) which target and compromise the PV [2]. ROP5 is encoded by a multi-gene variable family of pseudokinases and can directly bind to and induce allosteric changes in host IRGs [3], presenting them for phosphorylation by the ROP18 [4,5] and ROP17 parasite kinases [6]. The process of phosphorylation inactivates host IRGs, preventing them from assembling on the surface of the PV, which in turn allows the parasite to replicate [7,8]. Genetic variations in ROP5 and ROP18 largely explain parasite strain differences in mouse virulence [9–13], highlighting the importance of the IRG system in the control of *T. gondii* infection. IRGs also

regulate the recruitment of Guanylate-Binding Proteins (GBPs) and autophagy machinery to the PV membrane (PVM), both of which contribute to cell autonomous immunity to *T. gondii* [14,15].

Since IRGs and GBPs are induced transcriptionally following stimulation with IFN $\gamma$  [16], immune cells that produce IFN $\gamma$  are critically important for resistance to *T. gondii* [17]. CD8 T cell IFN $\gamma$  responses are required for host survival to *T. gondii* infections [18–21] and to prevent reactivation of the dormant form [22,23]. In vaccinated or chronically infected mice, IFN $\gamma$  and CD8 T cells are primarily responsible for protection against lethal secondary infections [24,25]. However, most *T. gondii* strains that express virulent alleles of ROP5 and ROP18 evade the host's immunological memory response and superinfect the brains of challenged survivors [26], implicating that sterile immunity to *T. gondii* may be difficult to achieve, as noted for other parasitic pathogens [27]. Whether *T. gondii* manipulates induction of the host's IFN $\gamma$  response to prolong its survival is unknown, but could represent a general strategy to promote persistence and latency, as noted for numerous viral pathogens in the presence of clonally expanded antigen-specific CD8 T cells [28].

In order for naïve CD8 T cells to become IFN $\gamma$  producers, they must first be activated by peptides derived from the host's MHC 1 antigen presentation pathway and then receive cues from the environment or other immune cells to differentiate into IFN $\gamma$ -producing cells. The question of MHC 1 antigen presentation for *T. gondii* antigens has largely been addressed using two experimental systems. One analyzes antigen-specific CD8 T cell responses to parasite strains expressing the model antigen, chicken ovalbumin (OVA) [29,30], and the other analyzes responses to *T. gondii* immune-dominant antigen GRA6, encoded by type II strains [31,32]. From these studies, it is appreciated that active cell invasion by *T. gondii*, rather than phagocytosis of invasion-blocked or heat-killed parasites, is required to stimulate host CD8 T cells [30,33,34]. The antigen must be in the parasite's secretory pathway [30,35], degraded by host cytosolic proteasomes [31,36], transported via the endoplasmic reticulum (ER) TAP1/2 translocon [29–31,34], and eventually loaded onto MHC 1 molecules. Although dense granules and rhoptry proteins access the host cytosol where MHC 1 antigen processing readily occurs, antigens targeted to the dense granule secretory pathway elicit a greater CD8 T cell response [35]. The PV is therefore a suitable platform for MHC 1 antigen presentation, which is remarkable given the PV of *T. gondii* does not initially fuse with host organelles [37,38], nor is contained within the conventional endocytic compartments of the cell.

The mechanism by which the immune system gains access to PV antigens of *T. gondii* has remained an active area of research, notwithstanding for its implication in vaccine development [39] and the ability of *T. gondii* to elicit anti-tumor responses [40]. In the case of *T. gondii* GRA6, it must be integrated in the PVM [41], where its C-terminal epitope [32] is exposed to the host cytosol [42] and degraded by unknown proteases. For the MHC 1 antigen presentation of transgenic OVA expressed in the PV lumen of *T. gondii*, two general mechanisms have been reported. Fusion between the PVM and the host ER [34], or ER-derived Golgi Intermediate Compartments (ERGICs) promotes OVA-specific CD8 T cell activation [43]. In this scenario, through a Sec22b SNARE-dependent mechanism, the host's MHC 1 antigen-processing machinery gains access to the PV whereby it shuttles parasite proteins into the cytosol for antigen processing. In a second mechanism, though not mutually exclusive, the PVM is compromised by the host's IRGs and selective autophagy systems therefore allowing OVA antigen release [30,44]. Via ROP5 and ROP18, *T. gondii* can bypass IRGs activity and presumably MHC 1 antigen presentation by sequestering OVA inside an intact PV [45]. However, several dense granule proteins are also implicated, signifying multiple non-redundant pathways may regulate MHC 1 antigen presentation of PV antigens [45]. Whether lessons learned from GRA6 and OVA extend to other antigens or parasite genetic backgrounds is unknown.

In addition to activation by antigen, CD8 T cells need proper co-stimulation [46,47] and cytokines, in particular IL-12 signaling, to fully commit to IFN $\gamma$  production during *T. gondii* infection [18,48,49]. In addition, IL-1 [50,51] and IL-18 can promote host survival during acute *T. gondii* infections [52], and are released following parasite detection and inflammatory activation by the pathogen sensors NLRP3 and NLRP1 [52–54]. Depending on the mode and time of infection, IL-1 and IL-18 can induce or repress inflammatory related pathologies in various tissues [55]. Inflammasome-matured IL-18 is important for IFN $\gamma$  production by CD4 T cells but is apparently dispensable for CD8 T cell IFN $\gamma$ -production during acute *T. gondii* infection [56]. Whether the inflammasome contributes to CD8 T cell activation or differentiation in different contexts or stages of *T. gondii* infection is unclear.

Given the parasite's need to establish latency and the host's dependence on CD8 T cells for immunity, we asked whether *T. gondii* has evolved to manipulate CD8 T cell IFN $\gamma$  responses to an endogenous antigen, and whether certain *T. gondii* genotypes are defined by their ability to induce or repress the production of this immune-protective cytokine. Through the use of T cell receptor transnuclear and IFN $\gamma$  reporter mice, host and parasite requirements were defined for the induction of IFN $\gamma$ -producing CD8 T cells to a conserved vacuolar antigen of *T. gondii*, TGD057. Here we report that TGD057-specific CD8 T cell responses are independent of the parasite's PV-export machinery, and like previous findings with OVA-engineered *T. gondii* strains, the IRG pathway is required. Multiple ROP5 isoforms suppress this response, including ROP5A which lacks a defined function or interaction with host IRGs. An analysis of parasite strains spanning twelve haplogroups suggests IFN $\gamma$  production is manipulated by *T. gondii* independent of any known IRG-ROP5 interaction or parasite virulence factor. Importantly, an NLRP3-dependent but inflammasome complex-independent pathway is required for inducing maximal CD8 T cell IFN $\gamma$  responses to *T. gondii* infected cells. Our findings point to novel host-parasite interactions by which IRGs and NLRP3 shape CD8 T cell IFN $\gamma$  responses to an intracellular pathogen.

## Results

### Naïve CD8 T cells respond to the vacuolar antigen TGD057 with a robust IFN $\gamma$ response

To determine host and parasite requirements for eliciting antigen-specific CD8 T cell responses to *T. gondii*, we took advantage of 'T57' transnuclear mice which were cloned from the nucleus of a single tetramer-positive *T. gondii*-specific CD8 T cell. T57 T cells from these mice have a single T cell receptor (TCR) specificity for the TGD057<sub>96-103</sub> epitope presented by H-2K<sup>b</sup> MHC 1 [49,57], and when adoptively transferred, confer resistance to infection with a type II strain [57]. TGD057 is a protein with unknown function but is predicted to be in the parasite's secretory pathway [58], and when deleted does not negatively impact parasite fitness, as inferred from a genome-wide CRISPR-CAS9 loss-of-function screen (phenotype score 2.1) [59], and from similar growth rates in tissue culture and plaque sizes observed between  $\Delta$ *tgd057* and parental strains. Importantly, *TGD057* (TG\_215980) is highly expressed ([ToxoDB.org](https://toxodb.org)) and the peptide epitope is conserved between strains (S1 Fig), facilitating comparative analyses of naïve CD8 T cell responses to parasite strains which may differ in immune modulation. In our experimental setup (i.e. the T cell activation 'T57 assay') (Fig 1A), bone marrow-derived macrophages (BMDMs) are infected with *T. gondii*, co-cultured with splenocytes and lymph node cells from naïve transnuclear T57 mice, and CD8 T cell activation markers or effector cytokines in the supernatant are measured. Reflecting early T cell activation events culminating in calcium-dependent NFAT activation of the IL-2 gene [60], this cytokine is produced as early as 24 hours post addition of T cells to parasite-infected BMDMs (Fig 1B).

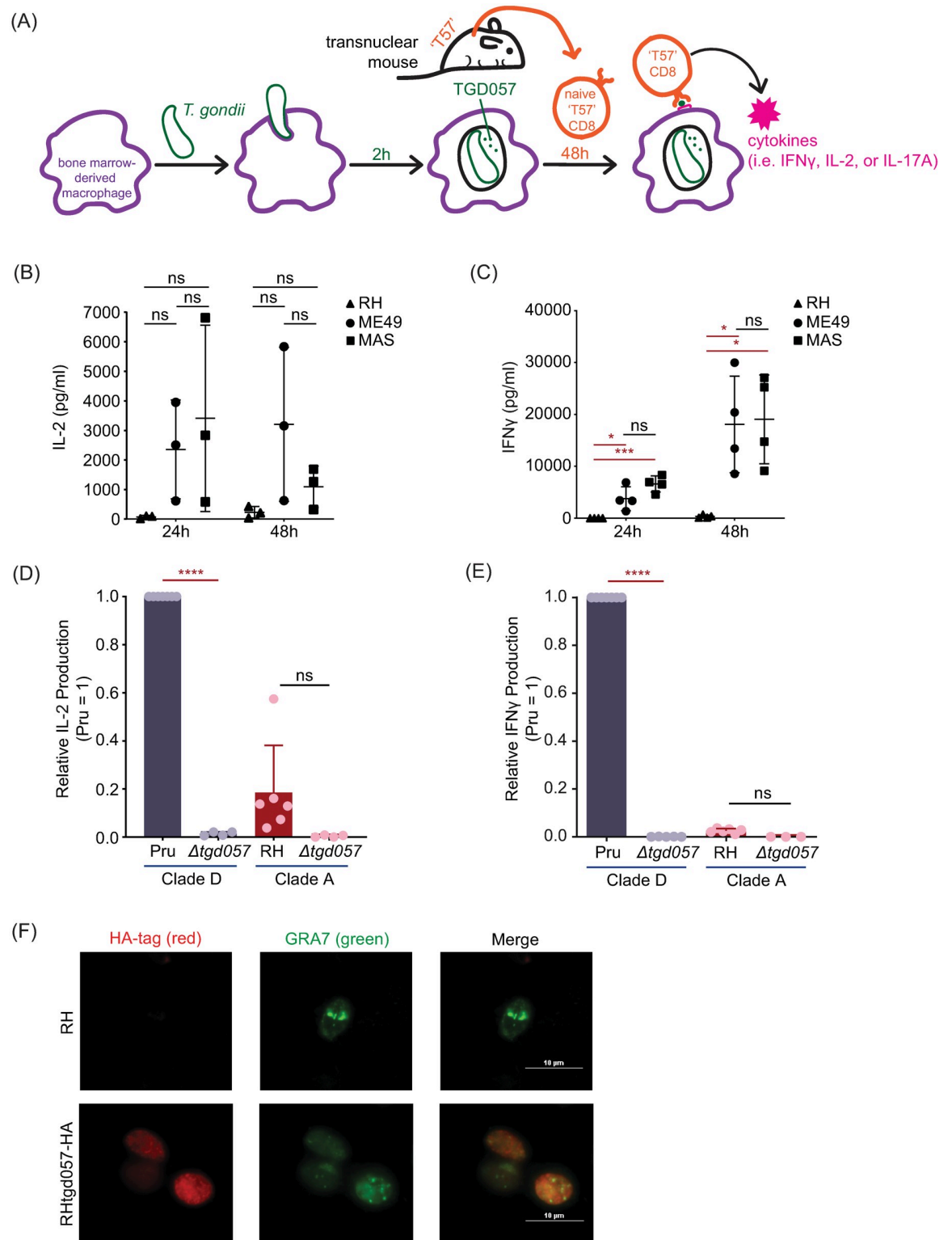


**Fig 1. A model to study naïve CD8 T cell responses to a *T. gondii* vacuolar antigen, TGD057.** (A) Schematic of the 'T57 assay'. Bone marrow-derived macrophages (BMDMs) are infected with *T. gondii* and 2h later, naïve T57 CD8 T cells obtained from transnuclear mice are added to the infected macrophages. T57 T cells bear antigen receptor specificity for a natural *T. gondii* antigen, the processed TGD057<sub>96-103</sub> peptide in complex with MHC 1 K<sup>b</sup>. Supernatant from the co-culture is then harvested and cytokine concentrations are analyzed by ELISA. (B-C) TGD057-specific CD8 T cell responses to *T. gondii*-infected macrophages were measured over time to the



indicated parasite strains. At 24h and 48h time points, IFN $\gamma$  and IL-2 was measured by ELISA. Average of 3–4 experiments + SD (standard deviation) is plotted; each dot represents the result from an individual experiment. Statistical analysis comparing parasite strain differences were performed by two-way ANOVA with Bonferroni's correction; \*  $p \leq 0.05$ , \*\*\*  $p \leq 0.001$ , ns non-significant. (D–E) Parental and  $\Delta$ tg $d057$  *T. gondii* strains were assayed for the CD8 T cell response as described in Fig 1A. T57 IFN $\gamma$  and IL-2 responses at 48h, analyzed by ELISA, are normalized to that of the clade D wildtype strain (Pru). Average of 3–5 experiments + SD is shown, each dot represents the results from an individual experiment. Statistical analysis between parental and knockout strains is performed by an unpaired t-test; \*\*\*\*  $p \leq 0.0001$ , ns non-significant. Clade assignments (clades A–F) are indicated for each strain as previously determined by population based genome-wide SNP comparisons and similar clustering of *T. gondii* strains [90]. (F) Human foreskin fibroblasts (HFFs) were infected with RH or an RH<sub>tg $d057$</sub> -HA endotagged strain. After 20 hours of infection, the samples were fixed, permeabilized and the tagged TGD057-HA was visualized in rat anti-HA antibodies, visualized in red. PVM is indicated by presence of the PVM integral and PV luminal dense granule protein, GRA7, visualized in green. A representative immunofluorescence image is shown.

<https://doi.org/10.1371/journal.ppat.1008327.g001>

In contrast and consistent with their naïve state, the T57 IFN $\gamma$  response develops with time, and is maximally detected at 48 hours (Fig 1C). Its magnitude is influenced by the parasite genotype, as evidenced by consistently high cytokine responses to the ME49 and MAS strains, and low responses to the RH strain (Fig 1B and 1C). *T. gondii* infection elicits strong CD8 T cell IFN $\gamma$  responses to TGD057 [49] and other antigens [61], as such IL-17 is only marginally detected in this system (S2A Fig). The measured phenotypes are antigen-specific, because the cytokine response is abolished in response to  $\Delta$ tg $d057$  strains which do not express the antigen (Fig 1D and 1E). Additionally, we noted that T57 CD8 T cells fail to upregulate the early activation marker CD69 in response to  $\Delta$ tg $d057$ . Previous observations from sub-cellular fractionation and immunofluorescence studies have identified TGD057 to be both within the PV of infected cells [41] and to the cytoskeleton region of the parasite [48]. Three-dimensional mass spectrometry LOPIT analysis (Location of Organelle Proteins by Isotype Tagging) posits TGD057 to dense granules but lacks a strict assignment to any one organelle, the latter observation being consistent with most cytoskeleton network associated proteins [62]. An endotagged RH<sub>tg $d057$</sub> -HA strain was generated and TGD057 is always found within PVM defined by GRA7 staining vacuoles (Fig 1F), demonstrating TGD057, in its natural state, stays inside the PV. In summary, the T57 system allows analysis of naïve CD8 T cell responses to an endogenous vacuolar antigen of *T. gondii*.

### TGD057 antigen acquisition is not dependent on the parasite's protein export pathway

To understand how *T. gondii* vacuolar antigens might escape from the vacuole and enter the host's MHC 1 antigen presentation pathway, the parasite's export machinery was explored. One way for vacuolar proteins to enter the host cytosol is through parasite-mediated export across the PV membrane (PVM). Dense granule proteins that reside within the PV can leave the vacuole through *T. gondii*'s export machinery, which includes the Golgi-resident protein aspartyl protease, ASP5 [63,64], and the PVM-integrated translocon protein MYR1 [65]. *T. gondii* ASP5 is an orthologue of *Plasmodium* protease Plasmepsin V which recognizes a *Plasmodium* export element (PEXEL) motif (RxLxE/Q/D) [66] and cleaves after the leucine (RxL↓xE/Q/D) preparing PEXEL-bearing proteins for export across the PVM into the host erythrocyte [67]. Like Plasmepsin V, *T. gondii* ASP5 recognizes and cleaves a PEXEL-like motif (RRL↓XX) (*Toxoplasma* export element or 'TEXEL' motif) [64], and its protease function is necessary for the export of all known exported PV proteins [68]. For example, GRA16 contains an RRL↓XX sequence, is cleaved by ASP5, and utilizes the MYR1 translocon complex for protein export [64,69]. Other GRAs including GRA24 [63,65] and TEEGR/HCE1 [70,71], while being fully dependent on ASP5 and MYR1 for their export, lack a functional TEXEL sequence. As TGD057 contains an RRL sequence, we hypothesized ASP5 and/or MYR1 may

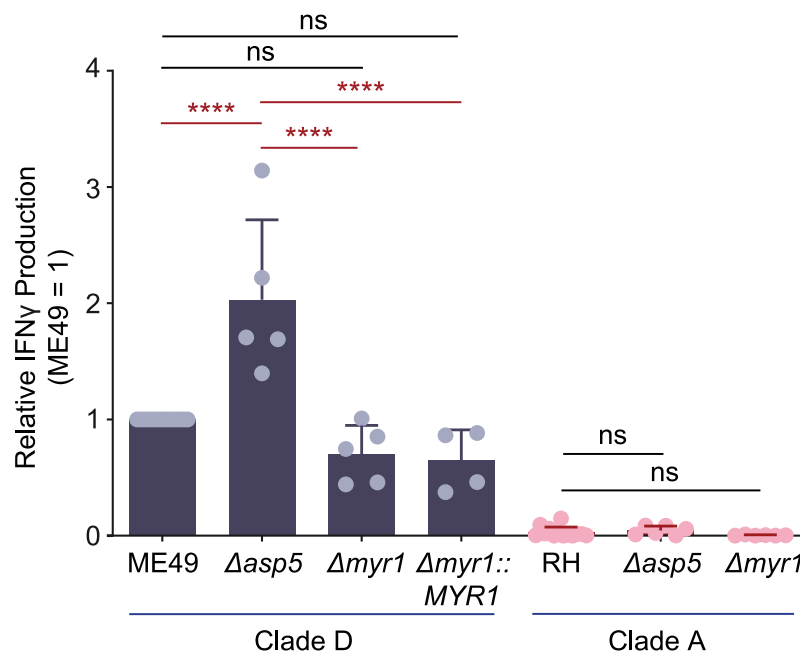


**Fig 2. TGD057-specific CD8 T cell IFN $\gamma$  responses do not require the parasite's export machinery.** The  $\Delta asp5$  and  $\Delta myr1$  *T. gondii* strains listed were assayed for host CD8 T cell responses as previously described in Fig 1A. The IFN $\gamma$  response at 48h, as analyzed by ELISA, is normalized to that of the clade D wildtype strain (ME49). Average of 4–6 experiments + SD is shown, each dot represents the results from one experiment. Statistical analysis was performed using one-way ANOVA with Bonferroni's correction comparing mutant to parental strains; \*\*\*\*  $p \leq 0.0001$ , ns non-significant.

<https://doi.org/10.1371/journal.ppat.1008327.g002>

be involved in the export of TGD057 from the PV, leading to MHC 1 antigen presentation and T57 antigen-specific CD8 T cell responses. To test this, the TGD057-specific CD8 T cell response to  $\Delta asp5$  and  $\Delta myr1$  strains was measured as previously described in Fig 1A. In contrast to the hypothesis, ME49  $\Delta asp5$  induced a higher CD8 T cell response compared to that of wildtype (WT) ME49 (Fig 2). Moreover, T57 responses to ME49, ME49  $\Delta myr1$  and *MYR1* complementation strains (ME49  $\Delta myr1::MYR1$ ) were comparable (Fig 2). Since the T57 cytokine response to the type I RH strain was uniformly low (Fig 1B and 1C), inferring requirements for export machinery using these parasite strains was uninformative. Nonetheless, CD8 T cell responses to the type II strain do not require ASP5 and MYR1, suggesting protein export from the PV is not necessary for MHC 1 antigen presentation of the vacuolar TGD057 antigen.

### CD8 T cell IFN $\gamma$ responses to TGD057 require host machinery downstream of the regulatory IRGs

Instead, we hypothesized the T57 CD8 T cell response requires PV disruption and is IRG-mediated, as implicated from studies of OT1 CD8 T cell responses, or hybridoma derivatives, to parasite strains that express the model OVA antigen in the PV lumen [45,72,73]. To this



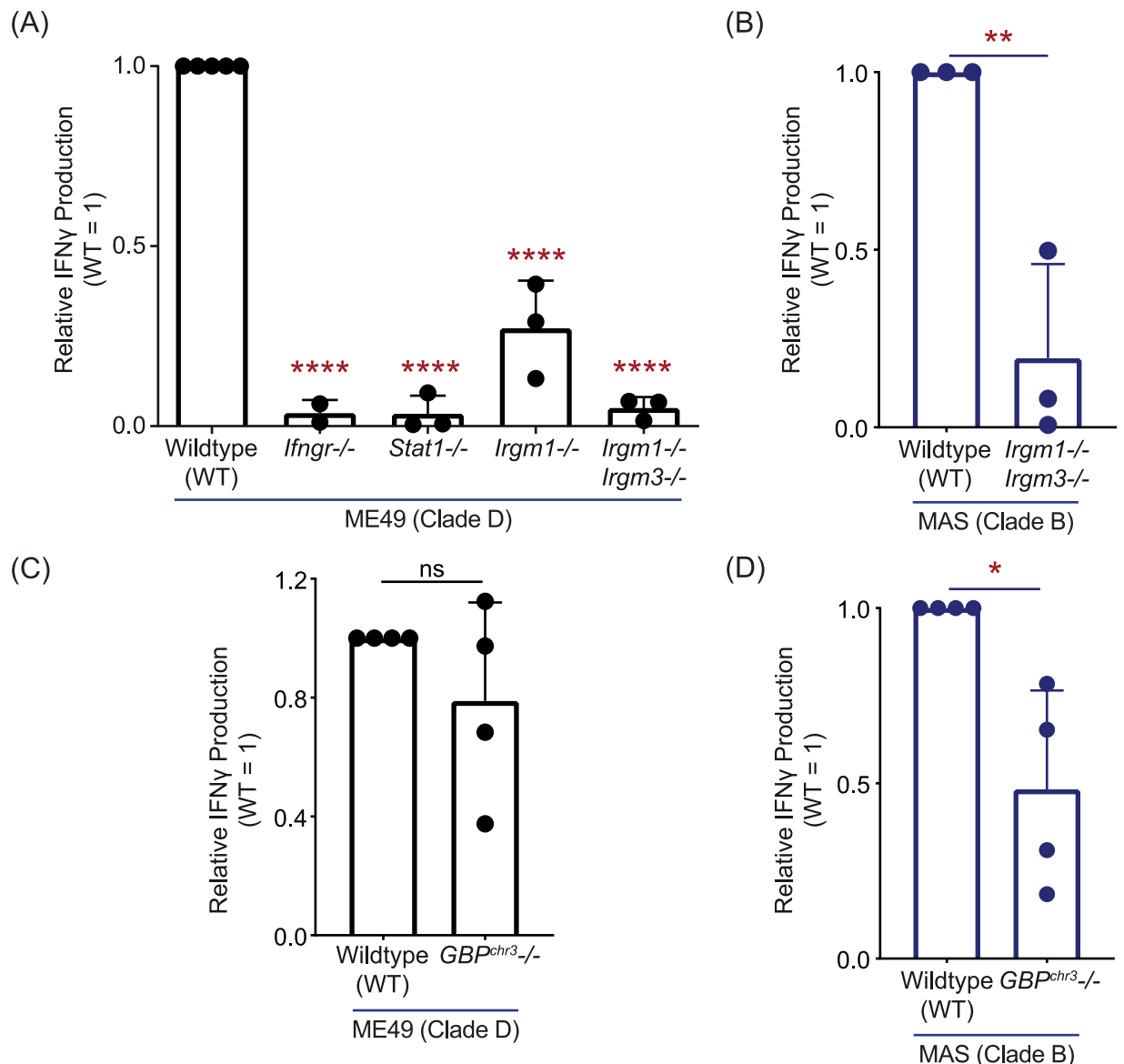


**Fig 3. TGD057-specific CD8 T cell IFN $\gamma$  responses are partially dependent on host GBPs but entirely dependent on regulatory IRGs.** (A,C) BMDMs with indicated gene deletion (-/-) were infected with the clade D ME49, or (B,D) clade B MAS strain. T57 T cell IFN $\gamma$  responses were analyzed by ELISA at 48h and normalized to the response elicited by infected wildtype (WT) BMDMs. Average of 2–4 experiments + SD is shown, each dot represents the result from an individual experiment. Statistical analyses were performed by one-way ANOVA with Bonferroni's correction (A) or unpaired two-tailed t-tests (B–D); \*  $p \leq 0.05$ , \*\*  $p \leq 0.01$ , \*\*\*\*  $p \leq 0.0001$ , ns non-significant.

<https://doi.org/10.1371/journal.ppat.1008327.g003>

end, T57 assays were performed with various BMDMs that are defective in IRG function. In the experimental setup, IFN $\gamma$  is derived from activated T57 cells and is predicted to induce IRG expression in WT but not *Stat1*<sup>-/-</sup> or *Ifngr*<sup>-/-</sup> macrophages. Consistent with this supposition, the TGD057-specific CD8 T cell response to the ME49 strain was nearly abolished in the absence of IFN $\gamma$ -STAT1 signaling (Fig 3A). In mice, there are 23 IRGs that can be separated into two subfamilies: 1) the effector IRGs (or 'GKS class' based on an amino acid motif in their GTP binding P-loop) and 2) the regulatory IRGs ('GMS class') [74]. Whereas effector IRGs bind the vacuolar membrane of the PV [75,76] and mediate membrane destruction via GTP hydrolysis [77], regulatory IRGs (or 'IRGMs') localize to host cellular organelles preventing

effector IRGs from destroying host membranes [78,79]. Regulatory IRGMs bind to effector IRGs keeping them in their GDP bound inactive state [80], in a manner similar to *T. gondii* ROP5 [3,4,81]. In the absence of IRGMs, effector IRGs fail to localize to pathogen PVs [80,82] and pathogen restriction is lost [83]. In mice there are three regulatory IRGs (IRGM-1, -2 and -3) and *Irgm1*<sup>-/-</sup> or *Irgm1/3*<sup>-/-</sup> double knockout macrophages were analyzed. Similar to the OVA system, the TGD057-specific CD8 T cell response to stimulatory parasite strains, such as type II ME49 and the atypical strain MAS, require the activity of regulatory IRGMs (Fig 3A and 3B). In addition, IFN $\gamma$ -inducible Guanylate-Binding Proteins (GBPs) localize to the PV in an IRGM-dependent manner [78] and mediate *T. gondii* resistance [15]. GBPs encoded on murine chromosome 3 (GBP<sup>chr3</sup>) are involved in PV disruption, promote effector IRG recruitment to the PV of *T. gondii* [73,84], and once compromised will attack the parasite's plasma membrane, decreasing its fitness [14]. To test whether GBPs are required for TGD057-specific CD8 T cell responses, GBP<sup>chr3</sup>-deficient BMDMs lacking *Gbp1*, *Gbp2*, *Gbp3*, *Gbp5*, and *Gbp7* were screened [73]. GBP<sup>chr3</sup> were not significantly involved in promoting TGD057-specific CD8 T cell IFN $\gamma$  responses to the ME49 strain (Fig 3C), but were partially required for the response to the atypical strain MAS (Fig 3D). Altogether, these observations are consistent with a model in which the PVM is compromised by host machinery downstream of regulatory IRGs, including GBPs [78] and likely other immunity genes, that mediate vacuolar antigen escape from the PV and entry into the host's MHC 1 antigen-presentation pathway.

### Multiple ROP5 isoforms of *T. gondii* suppress the CD8 T cell response to TGD057

Previous studies have shown that *T. gondii* virulence in mice is determined by parasite effectors that protect the PV from host immune attack. Specific alleles and isoforms of the rhopty pseudokinase ROP5 [3,5,9,12,13,85], ROP18 [4,7,10,81,86] and ROP17 kinases [4,81] encoded by virulent parasite strains, are noted for their ability to inhibit the destructive functions of IRGs at the PVM, including *Irgb6* and *Irga6* [2–4,80,81]. These rhopty proteins also impact the association of GBPs with the PV [84,87]. Thus, we reasoned the host CD8 T cell response to TGD057 would be antagonized by some or all of these secreted effectors. Indeed, when ROP5 is not expressed in the type I RH strain (clade A, RH  $\Delta$ *rop5*), the CD8 T cell IFN $\gamma$  and IL-2 response is robust (Fig 4, S3A Fig), and on average, the IFN $\gamma$  response is half of that elicited by the stimulatory type II strains (Fig 4). The ROP5 locus consists of ROP5A, ROP5B and ROP5C genes, which differ in copy number between strains, and is under diversifying selection [3,9,12,13,81,85]. ROP5B and ROP5C isoforms of virulent strains bind to and prevent accumulation of effector IRGs on the parasite's PVM, including *Irga6* and *Irgb6* [3,4,81], which are required for host resistance to primary infection [88,89]. In contrast, ROP5A lacks a defined host binding partner and function, but does promote virulence by an unknown mechanism that is sensitive to copy number. For example, increasing copy number of ROP5A from one to two copies promotes virulence of RH  $\Delta$ *rop5* complementation strains, whereas RH  $\Delta$ *rop5* +ROP5B+ROP5A phenocopies the virulence of the parental RH strain [9]. Therefore, a series of RH  $\Delta$ *rop5* strains complemented with one or two copies of ROP5B or ROP5A isoforms from clade A, or a single ROP5A isoform from the type II genetic background (clade D) was analyzed. Importantly, all RH  $\Delta$ *rop5*+ROP5 complementation strains phenocopied the T57 response to the parental RH strain (Fig 4). Since ROP5A inhibits the T57 IFN $\gamma$  response (Fig 4), we infer *Irgb6* and *Irga6* are likely not responsible for this phenotype because the ROP5A isoform does not inhibit *Irgb6* or *Irga6* coating of the PVM [4], nor *Irga6* oligomerization [3]. Consistent with this supposition, all ROP5A complementation strains failed to inhibit *Irgb6*-PV association (Fig 4B and 4C). Of note, the sequestosome-1 (p62) associates with the

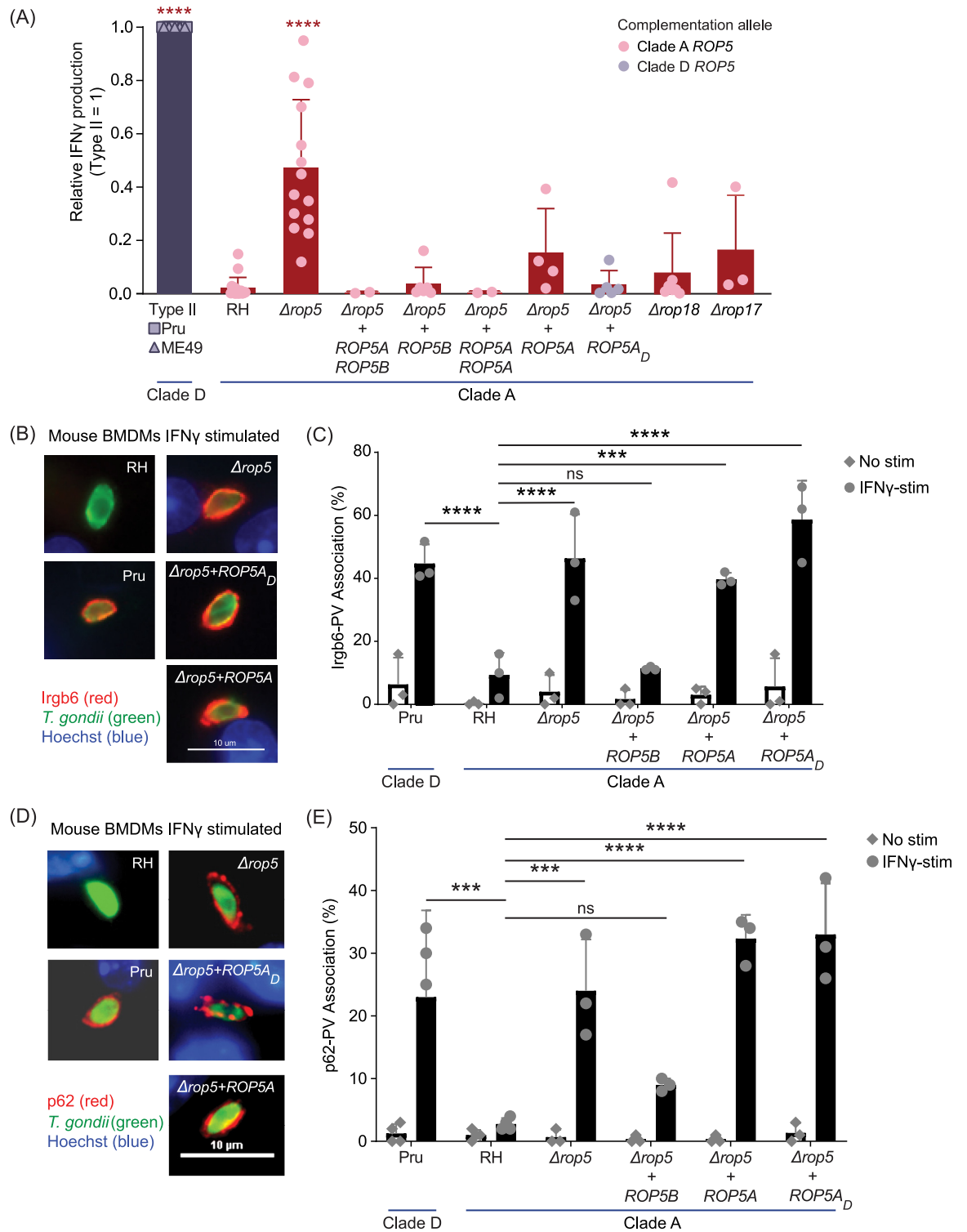


**Fig 4. Multiple ROP5 isoforms inhibit TGD057-specific CD8 T cell IFN $\gamma$  responses to *T. gondii*.** (A) T57 CD8 T cell IFN $\gamma$  responses to the RH and RH  $\Delta rop5$  strains, including various ROP5A and/or ROP5B complementation strains from clade A or from clade D (RH  $\Delta rop5 + ROP5A_D$ ), were analyzed as described in Fig 1A. Additionally, T57 IFN $\gamma$  responses to RH  $\Delta rop17$  and RH  $\Delta rop18$  strains were determined. IFN $\gamma$  was detected by ELISA at 48h and normalized to the response elicited by clade D strains, Pru ( $\square$ ) or ME49 ( $\Delta$ ). Average of 2–14 experiments + SD is shown, each dot represents the result from an individual experiment. Statistical analysis was

performed using one-way ANOVA with Bonferroni's correction comparing all strains to the RH strain, only type II and RH  $\Delta rop5$  strains proved significantly different from RH over multiple experiments; \*\*\*\*  $p \leq 0.0001$ . (B-E) Untreated or IFN $\gamma$ -stimulated BMDMs were infected with the indicated *T. gondii* strains. After 3–4 hours of infection, the samples were fixed and analyzed by fluorescence microscopy. *T. gondii* PVM was visualized in green with anti-GRA7 polyclonal rabbit antibodies and 100 vacuoles were quantified for each condition. (B) Representative images are shown of Irgb6-PV localization in parasite-infected IFN $\gamma$ -stimulated BMDMs. Irgb6-PV localization was visualized in red with anti-Irgb6 polyclonal goat antibodies, and (C) plotted as percent of total GRA7+ *T. gondii* vacuoles. Plotted is the average + SD of 3 experiments. Statistical analysis was performed using two-way ANOVA with Bonferroni's correction; \*\*\*  $p \leq 0.001$ , \*\*\*\*  $p \leq 0.0001$ , ns non-significant; shown are statistical comparisons to the RH parental strain. (D) Representative images are shown of p62-PV localization in parasite-infected IFN $\gamma$ -stimulated BMDMs. P62-PV localization was visualized in red with a mouse anti-p62 monoclonal antibody, and (E) plotted as percent of total GRA7+ *T. gondii* vacuoles. Plotted is the average + SD of 3–4 experiments. Statistical analysis was performed using two-way ANOVA with Bonferroni's correction; \*\*\*  $p \leq 0.001$ , \*\*\*\*  $p \leq 0.0001$ , ns non-significant; shown are statistical comparisons to the RH parental strain.

<https://doi.org/10.1371/journal.ppat.1008327.g004>

PV in an IFN $\gamma$ -induced IRGM-dependent manner to promote OT1 T cell responses to OVA-expressing *T. gondii* strains [44]. However, p62-PV association was not inhibited by ROP5A but instead phenocopied the PV-association patterns of Irgb6 (Fig 4D and 4E). Irgb6 has recently been shown to be required for p62-PV association in IFN $\gamma$ -stimulated cells, which is consistent with these observations [89]. The ROP18 [4] and ROP17 kinases [6] phosphorylate and inactivate Irga6 and Irgb6. Although there were slight increases in the T57 IFN $\gamma$  response to the RH  $\Delta rop17$  and RH  $\Delta rop18$  strains, these responses were not significantly different compared to that of the parental RH strain (Fig 4). Altogether, the data show that multiple ROP5 alleles and isoforms can suppress the T57 response to the TGD057 antigen, and this most likely by a mechanism independent of host Irgb6, Irga6 and p62 localization to the PV.

### ROP5-expressing clade A strains confer low TGD057-specific CD8 T cell IFN $\gamma$ responses

Due to the conserved nature of the TGD057 peptide epitope (S1 Fig), a unique opportunity arose to explore the development of CD8 T cell IFN $\gamma$  responses to multiple parasite strains spanning the genetic diversity of *T. gondii* [90]. Any observed trend between *T. gondii* virulence, genetic background, and the T cell response may offer clues to possible parasite immune modulation and adaptation to immune pressure incurred by CD8 T cells. Among the Eurasian clonal strains (types I, II, III) and North American isolates from haplogroups (HG) XI and XII, the virulent type I strains (GT1, RH) induced the lowest CD8 T cell response while intermediate virulent types II (Pru, ME49), XI (COUGAR) and XII (B73) and low virulent type III (CEP) strains, induced relatively high CD8 T cell IFN $\gamma$  (Figs 1C and 5A) and IL-2 responses (Fig 1B and S3B Fig). 'Atypical' strains, many of which are endemic to South America and highly virulent in laboratory mice (FOU, CAST, MAS, TgCatBr5, P89, GUY-MAT, GUY-DOS, GUY-KOE, RUB, and VAND), differed dramatically in eliciting T57 cytokine responses (Fig 5A and S3B Fig), signifying that parasite virulence is not a sole predictor of CD8 T cell activation. Instead a unique phenotypic pattern emerged, in which clade A strains (type I, HG VI and VII) [90] conferred low T57 cytokine responses while most other strains from clades B, C, D and F had potential to induce high cytokine responses (Fig 5A and S3B Fig). Consistent with previous results, T57 IFN $\gamma$  responses did not correlate with known Irgb6- and/or Irga6-PV associations of these strains. For example, a low percentage (~10%) of Irgb6 recruitment to the PV is observed for the MAS strain, yet a high CD8 T cell IFN $\gamma$  response is induced (Fig 5A), similar in magnitude to that of type II clade D strains (Figs 1C and 5A) whose PVs are highly decorated with Irgb6 (~45%) [81]. Even among highly virulent type I GT1 and Guyanan strains (i.e. GUY-KOE, GUY-MAT, GUY-DOS, VAND), where approximately 25% or less Irgb6-PV coating is observed [81], the CD8 T cell responses to these strains differ dramatically (Fig 5A and S3B Fig). Furthermore, one notable outlier among clade A strains is the relatively

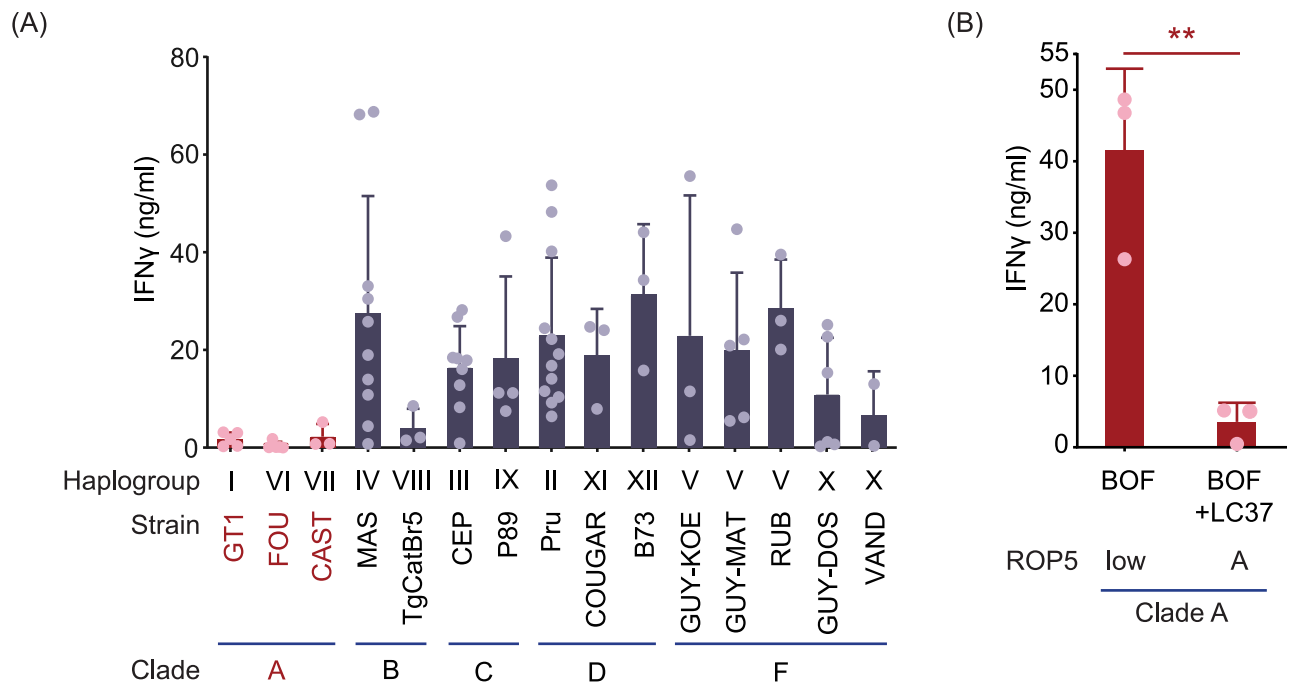


**Fig 5. Low CD8 T cell IFN $\gamma$  responses to ROP5-expressing clade A strains of *T. gondii*.** (A) The T57 CD8 T cell IFN $\gamma$  response to BMDMs infected with various *T. gondii* strains from most haplogroups (HG) were analyzed, including the clonal (types I-III), atypical (HG IV-X), and HG XI and XII strains. IFN $\gamma$  in the supernatant was measured by ELISA at 48h. Average of 2–12 experiments + SD for each strain is shown, each dot represents a single experiment. Statistical analysis is shown in S4 Fig. (B) The clade A BOF strain, which encodes a lowly expressed single *ROP5B* gene ('low') and BOF complemented with an LC37 cosmid that expresses the entire clade A *ROP5* locus ('A') were assayed as described in Fig 1A. Average IFN $\gamma$  detected in the supernatant at 48h of 3 experiments + SD is shown. Statistical analysis was performed by an unpaired two-tailed t-test; \*\*  $p \leq 0.01$ .

<https://doi.org/10.1371/journal.ppat.1008327.g005>

high T57 response to BOF (Fig 5B and S3B Fig). BOF encodes a single copy of *ROP5B* that is marginally expressed [81]. When BOF is complemented with the LC37 cosmid, which encodes the entire *ROP5* locus from the clade A type I genetic background, the CD8 T cell IFN $\gamma$  response is largely reduced (Fig 5B). We infer from these assays the clade A genetic background inhibits T57 IFN $\gamma$  responses, but the identity of the *ROP5*-host interacting partner and why this genetic background leads to repressed responses is currently unknown.

### Activation and IFN $\gamma$ differentiation of CD8 T cells are only partially inhibited by *T. gondii* ROP5

Following antigen-driven TCR stimulation (or 'signal 1'), early activated T cells receive secondary cues from the environment including co-stimulation ('signal 2') and cytokines ('signal 3') to commit to the production of cytokines such as IFN $\gamma$ . Whether clade A strains, through *ROP5* or other effectors, intersect one or several of these activation steps to lower T57 IFN $\gamma$  responses is unclear. To explore this issue further, we generated a 'T-GREAT' IFN $\gamma$  reporter mouse line by crossing T57 with GREAT mice [91]. GREAT mice report IFN $\gamma$  transcription with an internal ribosomal entry site (IRES)-eYFP reporter cassette inserted between the stop codon and endogenous 3'UTR with the poly-A tail of the *Ifng* gene. Without abrogating translation of IFN $\gamma$ , GREAT mice allow faithful detection of *Ifng* transcription via YFP fluorescence and flow cytometry [91]. In addition, surface expression of the activation marker CD69 is a proxy for early TCR signaling events, and is one of the first markers expressed by naïve T lymphocytes after activation [92]. In this way, the relative amount of TGD057 that has escaped the PV and ultimately presented by MHC 1 molecules can be inferred by T cell upregulation of

CD69, and this can be measured independently of IFN $\gamma$  transcription in T-GREAT cells. Naïve T-GREAT cells were co-cultured with BMDMs infected with RH (clade A), RH  $\Delta rop5$ , and ME49 (clade D) strains (Fig 6A), and the frequency of activated CD8 T cells (CD62L-CD69+ CD8+ T cells) (Fig 6B) as well as YFP levels (*Ifng*:YFP+ of CD62L-CD69+ CD8+ T cells) (Fig 6C) were measured by flow cytometry at 18 hours. Without parasite, few CD69+ or *Ifng*:YFP+ T-GREAT CD8 T cells were detected in the co-culture, consistent with their naïve beginnings (Fig 6B and 6C). In contrast and over a range of multiplicity of infections (MOIs), there was approximately three-fold more CD69+ CD8 T cells elicited by the ME49 compared to the RH strains (Fig 6B and 6D). Among T cells that have been activated (CD69+), a comparison of the *Ifng* transcript level revealed a six-fold increase in response to the ME49 compared to the RH strain (Fig 6C and 6E). Although removal of ROP5 enhances the activation and differentiation of T-GREAT cells to the RH  $\Delta rop5$  strain, *Ifng* transcript levels never equaled that elicited by ME49, especially at lower MOIs (Fig 6E). Therefore, the data show T57 cells do in fact recognize the RH strain, but once activated this genetic background fails to elicit other signals necessary for full induction of the T57 IFN $\gamma$  response. Moreover, the data implicate *T. gondii* genetic determinants other than ROP5 intersect CD8 T cell IFN $\gamma$  responses at the activation and likely differentiation steps.

### IFN $\gamma$ -production by TGD057-specific CD8 T cells does not solely depend on IL-12

IL-12 signaling is essential for IFN $\gamma$ -mediated control of *T. gondii* [93–95], and is required for full induction of IFN $\gamma$ -producing KLRG1+ effector CD8 T cells following *T. gondii* type II infections *in vivo* [48,49]. Moreover, the RH strain fails to induce robust IL-12 secretion in infected macrophages [96,97], perhaps underpinning the low T57 IFN $\gamma$  responses to clade A strains observed in this system. To understand what extent IL-12 influences IFN $\gamma$ -production, the T57 assay was performed with IL-12p40 deficient *Il12b*<sup>-/-</sup> BMDMs. The T57 IFN $\gamma$  response to ME49- (Fig 7A), or MAS-infected *Il12b*<sup>-/-</sup> BMDMs (Fig 7B) was reduced but not entirely abrogated compared to that of infected WT BMDMs. A partial reduction was also reported for adoptively transferred *Il-12 $\beta$ 2*<sup>-/-</sup> CD8 T cells that specifically lack IL-12 signaling during primary infection [48]. Next, the T57 assay was performed with parasite strains known to regulate host IL-12 production. Three *T. gondii* effector proteins—GRA15, GRA24 and ROP16—modulate IL-12 production in infected BMDMs [98–101]. Polymorphisms in GRA15 and ROP16 largely account for parasite strain differences in alternative (M2) and classical activation (M1) of macrophages [100]. Specifically, polymorphisms in GRA15 render type II strains able to activate the NF- $\kappa$ B pathway through direct association with TRAF2 and TRAF6 [102], and its expression is an absolute requirement for IL-12p70 [100] and largely responsible for IL-12p40 production by type II-infected BMDMs [98]. Through activation of host p38 MAPK, GRA24 promotes IL-12p40 and chemokine secretion by *T. gondii*-infected BMDMs [101]. Although no consistent difference between parental type II (Pru) and GRA15-deficient or GRA24-deficient strains was observed, T57 IFN $\gamma$  production was decreased but not abolished in response to a double deletion Pru  $\Delta gra15 \Delta gra24$  strain (Fig 7C). With respect to ROP16, in all *T. gondii* strains except those of clade D [103], the ROP16 kinase activates host STAT3, STAT5, STAT6 transcription factors [104–107], leading to the suppression of NF- $\kappa$ B signaling by an unknown mechanism [104,107]. When activating alleles of ROP16 are expressed as a transgene within the type II strain (Pru +*ROP16<sub>A</sub>*), it reduces IL-12 production in *T. gondii*-infected BMDMs and induces the expression of many M2 associated genes [100]. The T57 IFN $\gamma$  response to the Pru +*ROP16<sub>A</sub>* was reduced to half that of the parental strain (Fig 7D). Thus, although IL-12 and *T. gondii* GRA15, GRA24, and ROP16 have some impact in regulating TGD057-specific



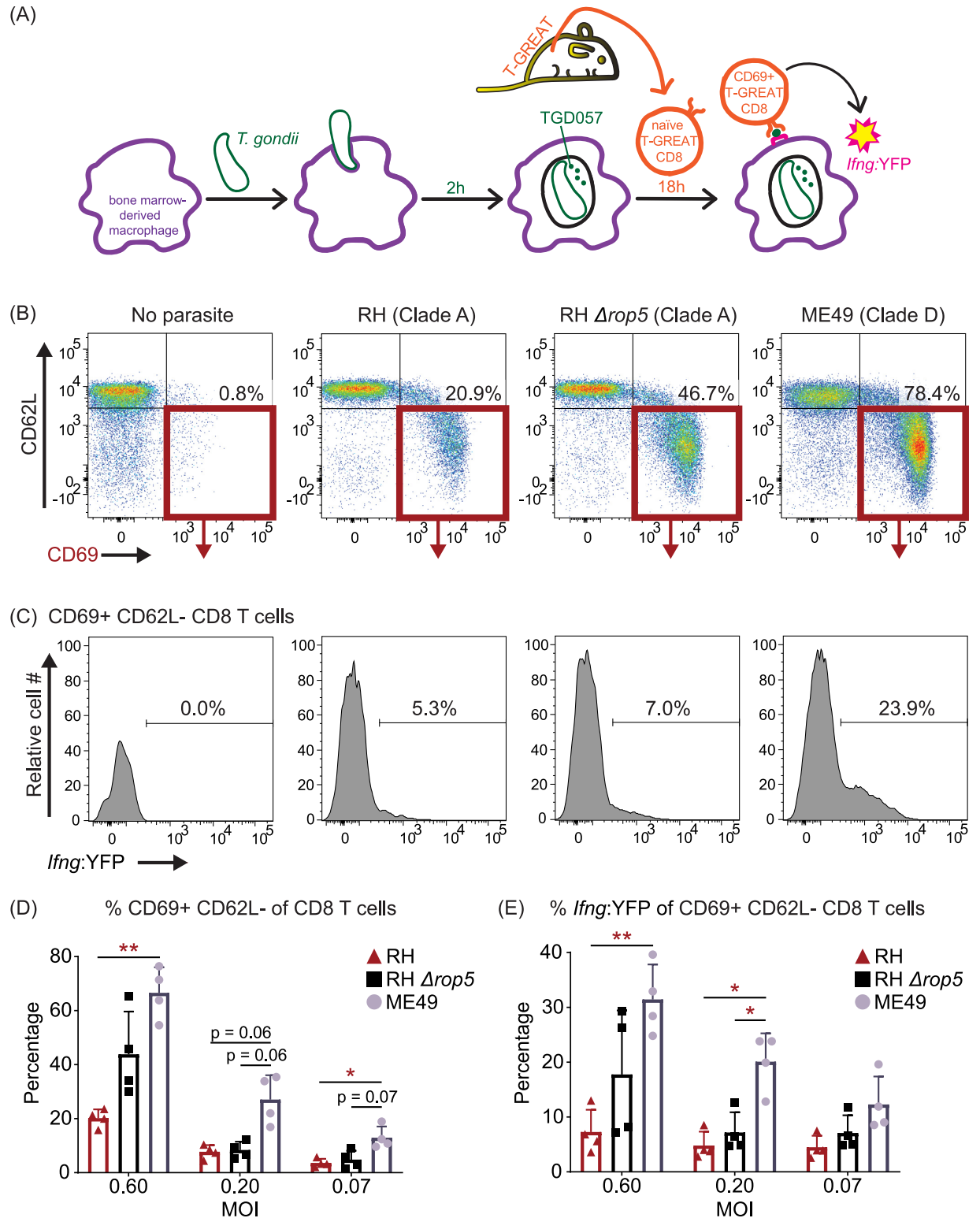


**Fig 6. In the absence of ROP5, clade A strains still inhibit TGD057-specific CD8 T cell activation and IFN $\gamma$  production.** (A) "T-GREAT" reporter mice were generated by crossing T57 mice with an IFN $\gamma$  (IRES)-eYFP reporter GREAT mouse line, which allows IFN $\gamma$  transcript levels to be measured by flow cytometry as a function of YFP expression. T-GREAT cells were analyzed for activation (CD69+) and IFN $\gamma$ -differentiation (*Ifng:YFP*+) in response to parasite-infected BMDMs at 18h. (B) The frequency of activated CD8 T cells (CD69+ CD62L- CD8+ T cells), as well as (C) the frequency of YFP+ (*Ifng:YFP*+) cells among activated CD69+ CD62L- CD8 T cells were compared between clade A

RH, RH  $\Delta rop5$ , and clade D ME49 strains. Representative flow plots with indicated gates and percentages are shown. (D) Percent CD69 + CD62L- of total CD8 T cells, and (E) percent *Irfng*:YFP+ of CD69+ CD62L- CD8 T cells are shown. Each dot represents the results of an individual experiment and plotted is the average + SD of 4 experiments. Statistical analyses were performed using two-way ANOVA with Bonferroni corrections; \*  $p \leq 0.05$ , \*\*  $p \leq 0.01$ .

<https://doi.org/10.1371/journal.ppat.1008327.g006>

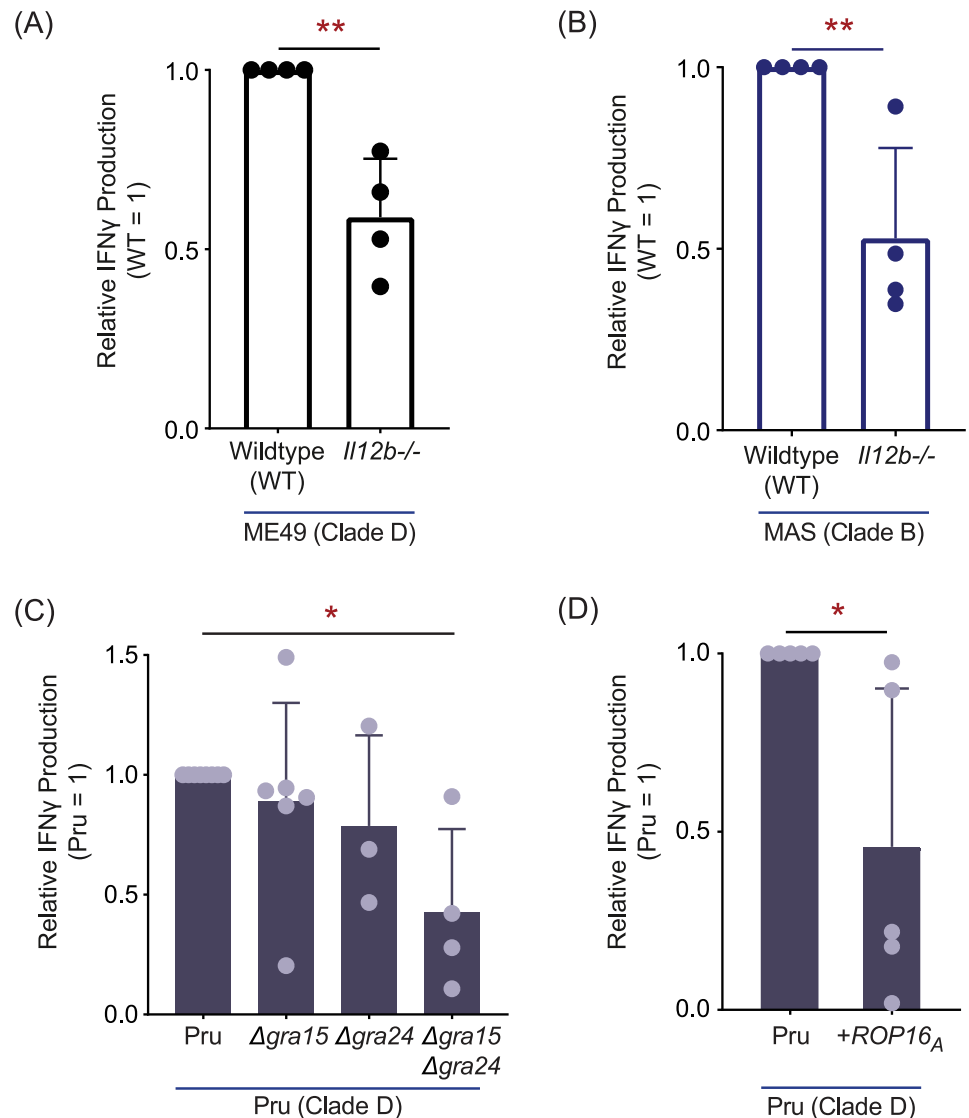


**Fig 7. IL-12 signaling is partially required for TGD057-specific CD8 T cell IFN $\gamma$  responses.** (A) *Il12b*<sup>-/-</sup> (IL-12p40) BMDMs were infected with clade D ME49, or (B) clade B MAS and TGD057-specific CD8 T cell IFN $\gamma$  responses were measured as described in Fig 1A. Each dot represents the result of an individual experiment and the average of 4 experiments + SD is shown; statistical analysis was performed with an unpaired two-tailed t-test; \*\*  $p \leq 0.01$ . (C) Various Pru (clade D) gene deletion strains,  $\Delta gra15$ ,  $\Delta gra24$ , and  $\Delta gra15 \Delta gra24$ , or (D) a Pru strain transgenically expressing clade A ROP16 (Pru +*ROP16*<sub>A</sub>) were assayed for TGD057-specific CD8 T cell IFN $\gamma$  responses. The IFN $\gamma$  response, as analyzed by ELISA, is normalized to that induced by the wildtype Pru strain. Each dot represents the result of an individual experiment and the average of 3–6 experiments + SD is shown. Statistical analysis was performed using one-way ANOVA with Bonferroni's correction for (C), and an unpaired two-tailed t-test for (D); \*  $p \leq 0.05$ .

<https://doi.org/10.1371/journal.ppat.1008327.g007>

CD8 T cell IFN $\gamma$ -production, the IL-12 axis does not fully account for IFN $\gamma$  commitment in this system.

### An inflammasome-independent NLRP3 pathway is required for maximal CD8 T cell IFN $\gamma$ responses to *T. gondii*

Both NLRP3 and NLRP1 inflammasome activation occur following *T. gondii* infection [52,53,108], and IL-1 and IL-18 are known regulators of IFN $\gamma$  production in a variety of cell types [109], including cells of the adaptive immune system [110]. Therefore, BMDMs deficient at various steps in the inflammasome activation cascade were analyzed. In brief, most NLRP proteins undergo ASC-driven oligomerization, causing auto-activation of caspase-1, that in turn lead to the cleavage and maturation of IL-1 $\beta$  and IL-18 [111]. Inflammasome activated caspase-1 and -11 also activate Gasdermin D, a key pore forming protein responsible for pyroptosis and extracellular release of IL-1/18 in several biological contexts [112–117]. The T57 IFN $\gamma$  response was largely reduced to parasite-infected *Nlrp1*<sup>-/-</sup> BMDMs, and completely absent to infected *Nlrp3*<sup>-/-</sup> BMDMs (Fig 8A and 8B). In contrast, the IFN $\gamma$  response was only partially decreased to *Asc*<sup>-/-</sup>, *Casp1/11*<sup>-/-</sup>, and *Gsdmd*<sup>-/-</sup> BMDMs infected with ME49 (Fig 8A), and no consistent difference was observed between knockout and WT BMDMs infected with MAS (Fig 8B). These results indicate CD8 T cell IFN $\gamma$  differentiation, though entirely dependent on NLRs, only partially involves inflammasome matured IL-1 and/or IL-18. Consistent with this supposition, the CD8 T cell IFN $\gamma$  response to parasite-infected macrophages is reduced but not abrogated in the absence of IL-18 and IL-1R-signaling, as assessed with neutralizing antibodies that block IL-1 $\beta$  and IL-1 $\alpha$  engagement with its receptor, IL-1R, and *Il18*<sup>-/-</sup> BMDMs (Fig 8C). Low levels of IL-1 $\beta$  and IL-18 detected in the co-culture may

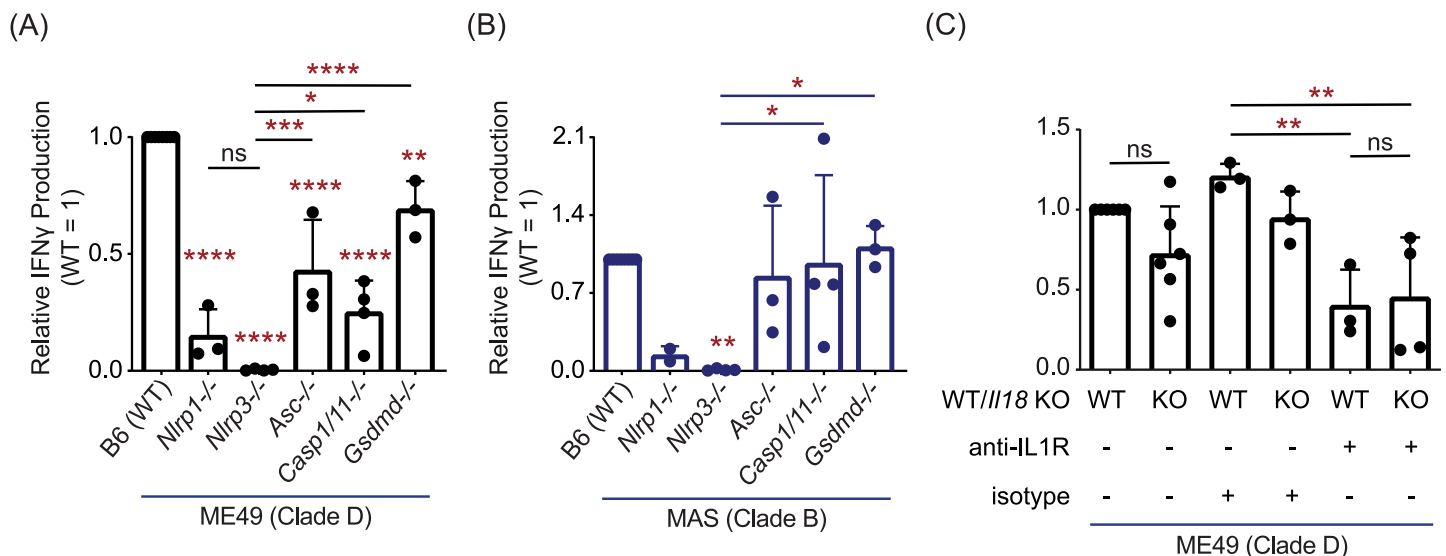


**Fig 8. An inflammasome-independent NLR pathway promotes CD8 T cell IFN $\gamma$  responses to *T. gondii*.** (A) BMDMs with indicated gene deletion (-/-) were infected with the clade D ME49, or (B) clade B MAS strain. The T57 CD8 T cell IFN $\gamma$  response to TGD057 was analyzed by ELISA and normalized to that of wildtype (WT) BMDMs. Each dot represents the result of an individual experiment, and the average of 2–4 experiments + SD is shown. Statistical analysis was performed using one-way ANOVA with Bonferroni's corrections compared to infected WT or *Nlrp3*<sup>-/-</sup> BMDMs, the latter comparisons are indicated with a line; \* p ≤ 0.05, \*\* p ≤ 0.01, \*\*\* p ≤ 0.001, \*\*\*\* p ≤ 0.0001, ns non-significant. (C) WT and *Il18*<sup>-/-</sup> BMDMs were infected with the clade D ME49 and assayed for CD8 T cell T57 IFN $\gamma$  production. Additionally, co-cultures were treated with either anti-IL-1R neutralization or isotype control antibodies. The IFN $\gamma$  level was measured by ELISA and normalized to that of untreated WT BMDMs. Each dot represents the results from an individual experiment and the average of 3–6 experiments + SD is shown. Statistical analysis was performed with one-way ANOVA and Bonferroni's corrections compared to untreated WT BMDMs; \*\* p ≤ 0.01, ns non-significant.

<https://doi.org/10.1371/journal.ppat.1008327.g008>

underscore the limited role these cytokines play in promoting IFN $\gamma$  responses in this system (S2B Fig).

Finally, to test whether NLRP3 impacts T cell activation or differentiation, T-GREAT CD8 T cell activation profiles to parasite-infected *Nlrp3*<sup>-/-</sup> BMDMs were explored. Whereas the percentage of early activated CD69<sup>+</sup> T-GREAT cells in response to ME49 and MAS infections was slightly decreased to *Nlrp3*<sup>-/-</sup> compared to WT BMDMs (Fig 9A), IFN $\gamma$  transcript levels in the activated CD69<sup>+</sup> population dropped by 50–70% (Fig 9B), suggesting NLRP3 induces a macrophage-derived signal required for IFN $\gamma$  transcription in activated CD8 T cells. Co-stimulation determines transcriptional regulation of IFN $\gamma$  in tumor-infiltrating T cells [118], and in its absence, enforces post-transcriptional silencing of IFN $\gamma$  in anergic self-reactive T cells [119], perhaps underscoring the blunted transcriptional (Fig 9B) and translational CD8 T cell IFN $\gamma$  response to parasite-infected *Nlrp3*<sup>-/-</sup> BMDMs (Fig 8). To determine whether NLRP3 regulates co-stimulatory pathways, a variety of co-stimulatory ligands and the PD-L1 inhibitory receptor were measured on infected BMDMs. As previously demonstrated for B7 family members CD80, CD86 [120], PD-L1 [100], and as demonstrated here, ICOSL, are readily induced on the surface of infected BMDMs (Fig 9C). Receptors and ligands of the TNF superfamily are also expressed transcriptionally following infection in BMDMs including CD70, CD40, OX40L and 41BBL [100], of which surface expression of OX40L appears most sensitive to induction by *T. gondii* infection (Fig 9C and S5B Fig). However, none of the measured receptors or ligands bore evidence for NLRP3-dependent regulation (Fig 9D and S5C Fig), nor does loss of NLRP3 influence MHC 1 K<sup>b</sup> expression (S5C Fig), as has been described for NLRC5-dependent induction of MHC class 1 genes [121]. To summarize, although inflammatory matured cytokines may play some role in promoting T57 IFN $\gamma$  production, there is no substitute for NLRP3, and to a similar extent NLRP1 in this system. Importantly, our data identify a novel NLR-dependent but NLR-ASC inflammasome complex-independent pathway that regulates CD8 T cell IFN $\gamma$  responses to an intracellular pathogen.

## Discussion

In this work, we set out to explore the role of parasite virulence factors, and host pathways that regulate CD8 T cell IFN $\gamma$  responses to an endogenous antigen. Given the close association between T cell activation and parasite-infected cells *in vivo* [33], and the immune pressure incurred by CD8 T cells, we reasoned there may be unidentified mechanisms governing host-pathogen interactions between *T. gondii* and this cell type. To this end, we used T57 transnuclear mice to develop a system to study this interaction, which has several advantages including the conserved nature of the TGD057 epitope and the ability to analyze the first moments of cytokine induction by an antigen-specific clonal CD8 T cell population with a normally expressed TCR. Without need for further antigen cloning, certain matters surrounding CD8 T cell IFN $\gamma$  differentiation and MHC 1 antigen presentation of TGD057 were revealed, including a fundamental role for *T. gondii* ROP5 and host NLRP3 in regulating this response. Our observations are both similar and divergent from results obtained in other systems, pointing to the contextual nature of immune responses to live pathogens, but also to new host mechanisms that possibly promote CD8 T cell immunity to *T. gondii*.

First, many similarities exist between the CD8 T cell response to TGD057 and OVA. For example, CD8 T cell activation to both antigens utilize the host's IRG system for optimal responses [30,44,45]. Such results indicate a need for the host to actively acquire antigens sequestered inside a PV [39]. We lend credence to this hypothesis, in that the parasite's export machinery appears dispensable for inducing TGD057-specific CD8 T cell responses (Fig 2). One curious observation in this regard, is that the TGD057 peptide epitope, SVLAFRRL,

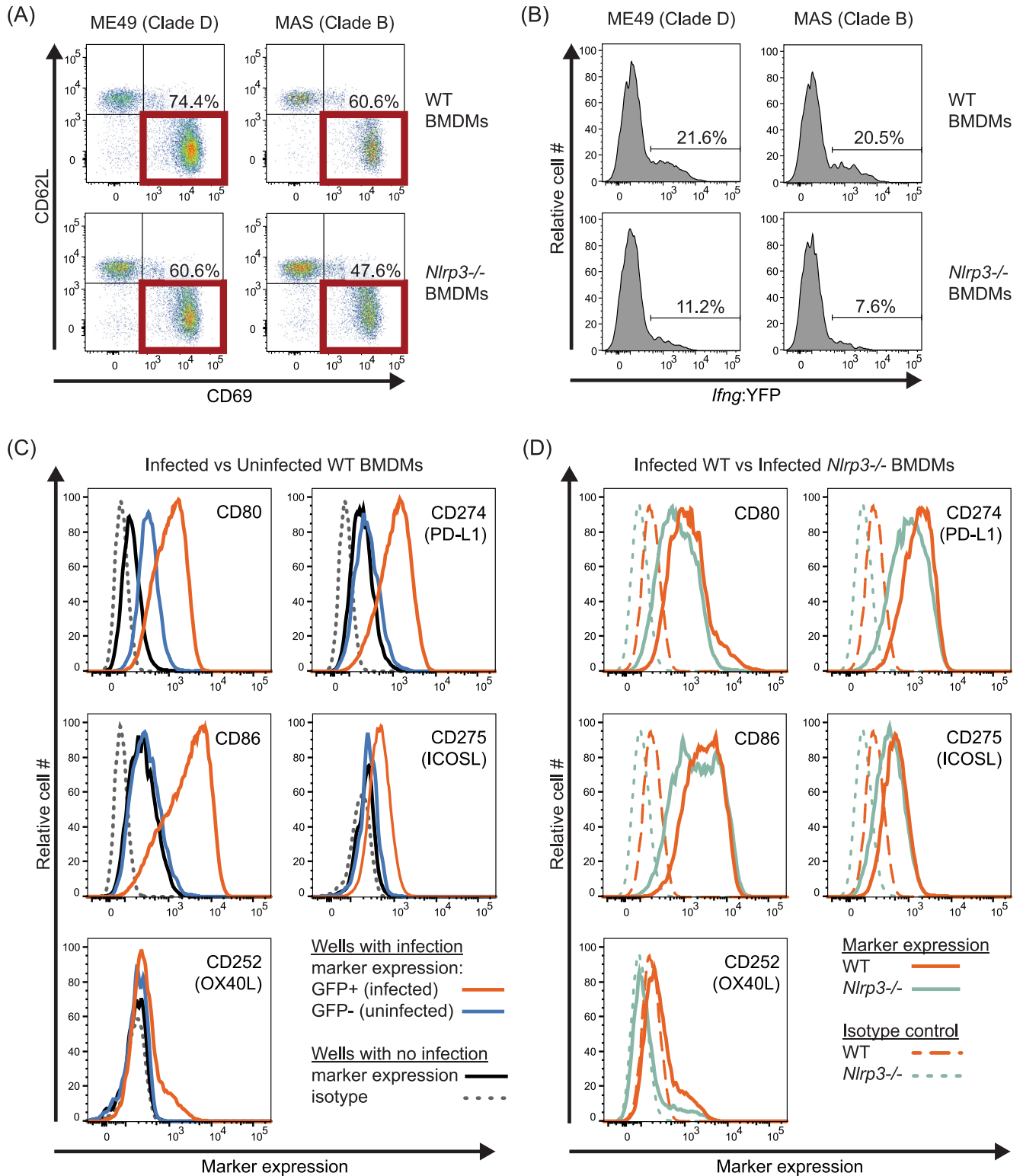


**Fig 9. Low IFN $\gamma$  transcriptional CD8 T cell responses to *T. gondii*-infected *Nlrp3*<sup>-/-</sup> BMDMs are not due to dysregulated co-stimulatory pathways.** (A-B) Wildtype (WT) and *Nlrp3*<sup>-/-</sup> BMDMs were infected with clade D ME49 or clade B MAS strains. T-GREAT CD8 T cell responses to parasite-infected BMDMs were analyzed as described in Fig 6A. (A) The frequency of activated CD8 T cells (CD69+ CD62L- CD8+ T cells), and (B) the frequency of YFP+ (*Ifng*:YFP+) cells among activated CD69+ CD62L- CD8 T cells were determined. Representative flow plots with indicated gates and frequencies are shown from 3–4 experiments. (C-D) WT and *Nlrp3*<sup>-/-</sup> BMDMs were infected with a GFP-expressing Pru strain (Pru A7) and stained for the indicated co

-stimulatory and -inhibitory molecules at 18h. (C) Surface marker expression of infected (GFP+) and uninfected (GFP-) WT BMDMs from an infected well, and of BMDMs from uninfected control wells are all compared in a single histogram plot; the isotype staining control is also indicated. A representative histogram plot from 2–3 independent experiments is shown for each marker. The gating strategy is depicted in S5A Fig. (D) As in C, but infected WT and *Nlrp3*<sup>-/-</sup> BMDMs (GFP+) are compared; isotype staining control of infected cells is also indicated. A representative histogram plot of 2–3 independent experiments is shown for each marker.

<https://doi.org/10.1371/journal.ppat.1008327.g009>

encodes the lone putative ASP5 recognition TEXEL motif in this protein (underlined) (S1 Fig). In fact, ASP5 cleavage would preferentially produce parasite peptides with a terminal leucine, which is the preferred anchor residue of the P8/9 peptide binding pocket of MHC 1 K<sup>b</sup> [122] and many other murine MHC and human HLA alleles. We initially thought ASP5 might prepare *T. gondii* antigens for binding host MHC 1 molecules, such that in the absence of ASP5, a blunted CD8 T cell response would ensue. Rather, the opposite occurred (Fig 2), ruling against parasite-assisted antigen processing of TGD057. However, beyond containing an RRL sequence, there is no evidence that TGD057 is actually cleaved by ASP5. Studies that utilized unbiased mass-spectrometry approaches to discover the repertoire of *T. gondii* proteins cleaved by ASP5 have failed to detect TGD057 as a substrate [123]. Moreover, of the over 300 mass spectra counts assigned to TGD057 from several proteomics studies (ToxoDB.org), not a single TGD057 peptide contains an intact RRL or TTSA sequence (C-terminal to the RRL). For known dense granules cleaved by ASP5, the protein migrates at a lower molecular weight than predicted and often two or more species can be observed by western blot analysis, including that of GRA7, GRA16, GRA19 [63], IST [124], MYR1 [64], LCAT, GRA44, GRA45, GRA46, and WNG2 [123]. In the original characterization of TGD057, using polyclonal rabbit serum generated against recombinant TGD057, only one band of predicted size (21 kDa) was observed [58]. In addition to its role in protein export, ASP5 is required for targeting dense granules to the PVM [63,64,125]. GRA6 association with the PVM significantly enhances its entry into the host's MHC 1 antigen presentation pathway, yet TGD057 is detected only in the non-membranous and soluble fraction of the PV [41]. Whether TGD057 sub-localization inside the PV impacts entry into the host's MHC 1 antigen presentation pathway is currently unknown. The enhanced response to the type II  $\Delta asp5$  strain (Fig 2) may also reflect decreased parasite fitness observed for this strain [63], or the role of an unidentified ASP5-targeted and PVM-associated GRA that inhibits CD8 T cell activation. Such possibilities await experimental validation.

Second, since *T. gondii* defends itself from immune attack by its virulence factor ROP5, this strategy affords a second benefit, the hiding of its vacuolar antigens from the host's MHC 1 antigen processing machinery. For TGD057, this battle is uniquely defined by ROP5A that has no known interacting partner, but suppresses the CD8 T cell response to TGD057. We predict this occurs by a mechanism independent from any known ROP5-IRG interaction. For example, ROP5B and ROP5C from clade A strains are able to prevent accumulation of effector IRGs on the parasite's PVM, including Irgb10, Irga6 and Irgb6, but this is not a function of clade A ROP5A [3,4], nor is this a known function for any ROP5 isoforms from clade D. Although ROP5C was not tested here, recently an OVA-expressing RH  $\Delta rop5$  +*ROP5C* strain was generated and CD8 T cell activation was partially inhibited by this strain [45]. Whatever mechanism underlies the ability of ROP5 to inhibit CD8 T cell activation, we hypothesize that it is controlled by ROP5A and ROP5B isoforms, and less so by ROP5C. Amino-acids in the 346–370 region in the IRG binding interface of ROP5 [3] can be found that distinguish clade A ROP5C from ROP5A and ROP5B of clades A and D. Whether these amino acids define a novel interaction with a less-studied effector IRG, of which there are 13 functional effector IRGs encoded in the C57BL/6 genome [126], or another host protein is currently unknown.



It is likely there is no single host-parasite interaction that determines antigen presentation for all *T. gondii* vacuolar antigens. For example, one notable difference between CD8 T cell responses to the vacuolar TGD057 and OVA antigens, is the role of the *T. gondii* ROP18 kinase. The CD8 T cell response to OVA appears largely inhibited by ROP18 [45], but at best, ROP18 plays a marginal role in this system (Figs 4 and S3A). These observations imply effector IRG modulation or the ATF6 $\beta$  ER-stress response, which is known to regulate CD8 T cell IFN $\gamma$  responses to *T. gondii* and is directly antagonized by the kinase activity of ROP18 [127], might be more important for CD8 T cell detection of OVA than TGD057. Furthermore, p62 is required for OVA-specific OT1 CD8 T cell activation by a mechanism that includes binding to ubiquitin-tagged PVs in IFN $\gamma$ -stimulated cells [44]. P62 recruits GBPs to the vacuole of *T. gondii* [128], suggesting GBPs may also assist in MHC 1 antigen presentation, for which we found some evidence (Fig 3C and 3D). Although the role of p62 using mouse knockout cells was not directly tested, a comparison of p62-PV localization patterns between stimulatory and non-stimulatory parasites strains (Fig 4D and 4E) argues against a dominant role for this pathway in our system. Other differences include lessons learned from the GRA6 antigen. When the C-terminal GRA6 epitope is facing the host cytosol it is highly stimulatory to CD8 T cells [42]. The protruding nature of the GRA6 epitope into the host cytosol may bypass need for host recruitment of IFN $\gamma$ -induced IRG/GBP machinery, thus facilitating its immuno-dominance. However, TGD057 is not an integral membrane protein nor is it associated with the membranous fractions of the PV [41]. It is therefore unclear how the initial antigen is first detected to start T57 IFN $\gamma$  responses, which paradoxically require IFN $\gamma$  signaling to begin with (Fig 3). A clue may come from the OVA system. Host derived ERGICs fuse with the PVM in a Sec22b SNARE-dependent process to initiate MHC 1 presentation of *T. gondii* expressed OVA [43]. Whether this pathway seeds the initial antigen-specific response to TGD057 is unknown. Yet even in response to clade A strains, which are poor inducers of TGD057-specific CD8 T cell IFN $\gamma$  and IL-2 responses (Fig 5 and S3B Fig), the early activation marker CD69 was readily detected on T57 CD8 T cells (Fig 6). The immune system is therefore robust in its ability to perceive *T. gondii* antigens, which employs multiple non-redundant pathways to acquire antigens from vacuolated pathogens [129].

Third, our studies demonstrate an absolute requirement for the pathogen sensor NLRP3, and to a similar extent NLRP1, for promoting naïve TGD057-specific CD8 T cell IFN $\gamma$  responses to parasite-infected cells. Moreover, it appears NLR-mediated regulation can occur in the absence of other components of the inflammasome cascade. This is inferred because T57 IFN $\gamma$  production was still detected in response to parasite-infected ASC, caspase-1/11, and gasdermin D deficient cells, or when IL-1/18 cytokine signaling was inhibited. In contrast, when NLRP3 is removed, there was no IFN $\gamma$  response (Fig 8), even though the CD8 T cells were activated (Fig 9). NLRs have several inflammasome independent functions, including the ability to form a bridge between ER and mitochondria to initiate inflammasome signaling [130]. NLRs also bind to and directly activate transcription factors, such as IRF4 [131] and the RFX complex [121], the latter induces MHC 1 expression [132]. Our results diverge from a recent report exploring the role of inflammasome components in promoting CD8 T cell IFN $\gamma$  responses during primary *T. gondii* infection. NLRP3, ASC and caspase 1/11 deficiency had no bearing on the frequency of peritoneal or splenic IFN $\gamma$ + CD8 T cells during primary *T. gondii* infection [56]. Certainly, CD8 T cells receive environmental cues *in vivo* that compensate for the lack of the inflammasome pathway, but are missing in our system. Given the diminished IFN $\gamma$ -transcriptional response to infected NLRP3-deficient cells (Fig 9) and the role co-stimulation plays in regulating T cell IFN $\gamma$  responses, we hypothesized co-stimulatory pathways were dysregulated in *Nlrp3*<sup>-/-</sup> infected cells, but this was not the case. Current studies are

underway to understand the mechanism by which NLRP3 deficiency impacts transcriptional and translation regulation of IFN $\gamma$  in activated CD8 T cells.

Finally, we present evidence that *T. gondii* strains differ in their ability to modulate CD8 T cell IFN $\gamma$  responses, which in theory might aid the parasite's survival in a broad host range. For example, T57 IFN $\gamma$  cell responses were low to *ROP5*-expressing clade A strains, which we hypothesized might be due to polymorphisms unique to clade A *ROP5* alleles. However, both clade D and A *ROP5* alleles were equally able to repress the CD8 T cell IFN $\gamma$  response (Fig 4), indicating another polymorphic regulator is in effect. Our current work searching for this polymorphic modulator of host CD8 T cell IFN $\gamma$  response has revealed no genotype-phenotype correlation at the *ROP5* locus. Instead, the polymorphic regulator could intersect CD8 T cell differentiation, for example through modulation of the host's NLRs, or antigen release, possibly by assisting the function of ROP5A. Given the enhanced T cell response to the ME49  $\Delta$ *asp5* strain, ASP5 may target a polymorphic dense granule to the PVM that represses the response. Recently, Rommereim *et al.* has shown that OVA-specific CD8 T cell activation is regulated by multiple GRA(s) [45]. Whether any such GRA is responsible for the observed strain differences in T57 activation require further investigation.

In summary, since any warm-blooded animal can serve as an intermediate host for *T. gondii*, the parasite may have difficulty achieving stable chronic infections in every animal to promote its transmission. This is evidenced by the observation that *T. gondii* strains differ dramatically in virulence in laboratory mice [133] and correlate with the severity of human toxoplasmosis [134–137]. This led to the hypothesis that parasite strains have adapted to certain intermediate host niches [138], defined by host genetics, including that of the murine IRG locus [126]. This adaptation may also necessitate the manipulation of host adaptive immune responses. Here, we present evidence that *T. gondii* may direct CD8 T cell IFN $\gamma$  response for its advantage. Perhaps NLRP3 and the MHC 1 antigen presentation pathway serve as two distinct sites for immune pressure, leading to the evolution of novel parasite virulence factors. Nevertheless, a closer and detailed understanding of the interactions between *T. gondii* and host CD8 T cells will eventually help us find potential therapeutic targets for toxoplasmosis, as well as to understand why *T. gondii* has spread so extensively.

## Materials and methods

### Ethics statement

All animal protocols were approved by UC Merced's Committee on Institutional Animal Care and Use Committee (IACUC) (AUP17-0013). All mouse work was performed in accordance with the recommendations in the *Guide to the Care and Use of Laboratory Animals* of the National Institutes of Health and the Animal Welfare Act (assurance number A4561-1). Inhalation of CO<sub>2</sub> to effect of 1.8 liters per minute was used for euthanasia of mice.

### Parasites

Tachyzoites of *Toxoplasma gondii* strains were passaged in 'Toxo medium' [4.5 g/liter D-glucose in DMEM with GlutaMAX (Gibco, cat#10566024), 1% heat-inactivated fetal bovine serum (FBS) (Omega Scientific, cat#FB-11, lot#441164), 1% penicillin-streptomycin (Gibco, cat#15140122)], in confluent monolayers of human foreskin fibroblasts (HFFs). HFFs were cultured in 'HFF medium' [4.5 g/liter D-glucose in DMEM with GlutaMAX (Gibco), 20% heat-inactivated FBS (Omega Scientific), 1% penicillin-streptomycin (Gibco), 0.2% Gentamicin (Gibco, cat#15710072), 1X L-Glutamine (Gibco, cat#21051024)]. Strains assayed include GT1 (type I, clade A), BOF (Haplogroup "HG" VI, clade A), FOU (HG VI, clade A), CAST (HG VII, clade A), MAS (HG IV, clade B), TgCatBr5 (HG VIII, clade B), CEP *hxgpri*- (type

III, clade C), P89 (HG IX, clade C), ME49 *Δhxpprt::Luc* [139] (type II, clade D), Pru *Δhxpprt* (type II, clade D), COUGAR (HG XI, clade D), B73 (HG XII, clade D), GUY-KOE (HG V, clade F), GUY-MAT (HG V, clade F), RUB (HG V, clade F), GUY-DOS (HG X, clade F), and VAND (HG X, clade F). Other strains used include BOF+LC37 [81], RH *Δhxpprt* [140], RH *Δhxpprt Δku80* [141], RH *Δhxpprt Δku80 Δrop5::HXGPRT* (RH  $\Delta$ rop5) [9], RH *Δhxpprt Δku80 Δtgd057::HXGPRT* (RH  $\Delta$ tgd057) [26], RH *Δhxpprt Δku80 TGD057-HA::HXGPRT* (RH<sub>tgd057</sub>-HA) (generated here), Pru *Δhxpprt Δku80*, Pru *Δhxpprt Δku80 Δtgd057::HXGPRT* (Pru  $\Delta$ tgd057) (generated here), Pru A7 *Δhxpprt::gra2-GFP::tub1-FLUC* (Pru A7) [142], Pru A7 *Δhxpprt Δgra15::HXGPRT* (Pru  $\Delta$ gra15) [98], Pru A7 *Δhxpprt Δgra24* (1E9) (Pru  $\Delta$ gra24) (generated here), Pru *Δhxpprt Δgra15 Δgra24* (1F8) (Pru  $\Delta$ gra15  $\Delta$ gra24) (generated here), Pru A7 *Δhxpprt +ROP16<sub>A</sub>::HXGPRT* (Pru +ROP16<sub>A</sub>) [100], RH *Δhxpprt Δmyr1::HXGPRT* (RH  $\Delta$ myr1) [125], and RH *Δku80 Δasp5-ty::DHFR* (RH  $\Delta$ asp5) [69]. ME49 *Δasp5::DHFR* (ME49  $\Delta$ asp5) was a generous gift from Dominique Soldati-Favre (University of Geneva) [63]. ME49 *Δhxpprt::Luc Δmyr1::HXGPRT* (ME49  $\Delta$ myr1), ME49 *Δhxpprt::Luc Δmyr1 +MYR1-HA::HXGPRT* (ME49  $\Delta$ myr1::MYR1) [65], and RH *Δhxpprt Δrop17::HXGPRT* (PCRE) (RH  $\Delta$ rop17) [143] were generous gifts from John Boothroyd (Stanford University). The ROP5 complementation strains used in this study are as followed: RH *Δhxpprt Δku80 Δrop5 +ROP5A<sub>II-ME49</sub>His6-3xFlag* (C1A6) (RH  $\Delta$ rop5 +ROP5A<sub>D</sub>) (generated here), RH *Δhxpprt Δku80 Δrop5 +ROP5B<sub>III-CTG</sub>-His6-3xFlag* (H2) (RH  $\Delta$ rop5 +ROP5B) (generated here), RH *Δhxpprt Δku80 Δrop5 +ROP5A<sub>III-CTG</sub>His6-3xFlag* (C1B1) (RH  $\Delta$ rop5 +ROP5A), RH *Δhxpprt Δku80 Δrop5 Δuprt::ROP5A<sub>III</sub>-HA +ROP5B<sub>III-CTG</sub>-His6-3xFlag* (AC11) (RH  $\Delta$ rop5 +ROP5A +ROP5B), RH *Δhxpprt Δku80 Δrop5 Δuprt::ROP5A<sub>III</sub>-HA +ROP5A<sub>III-CTG</sub>-His6-3xFlag* (AA12) (RH  $\Delta$ rop5 +ROP5A+ROP5A) [9].

### Generation of gene knock-in and knockout parasite strains

The Pru *Δhxpprt Δku80 Δtgd057::HXGPRT* strain was generated using the same primers and strategy as previously described [26]. The RH *Δhxpprt Δku80 TGD057-HA::HXGPRT* endo-tagged strain was generated as previously described [144]. In brief, for endogenous tagging [141] of TGD057 with an HA tag, the gene (*TGGT1\_215980*) was amplified with a forward primer internal to the ATG start site of *TGD057* ["AC\_tgd057endoF2" 5'-CACCAACTACGTCGGAGCGCCTGTACG-3'], containing a 5'-CACC-3' sequence required for directional TOPO cloning in pENTR/D-TOPO (Invitrogen), and a reverse primer ["Tgd057 R HA stop" 5'-TTACGCGTAGTCCGGGACGTCGTACGGTACTCGACCTCAATGTTGTATTC-3'], containing the hemagglutinin (HA) tag sequence (underlined) followed by a stop codon. The resulting TGD057 HA-tagged DNA fragment was then cloned into the pTKO-att parasite expression vector [98] by Gateway Recombination Cloning Technology (Invitrogen). The resulting vector was linearized and transfected into RH *Δhxpprt Δku80* parasites by electroporation in a 2 mm cuvette (Bio-Rad Laboratories) with 2 mM ATP (MP Biomedicals) and 5 mM glutathione (EMD) in a Gene Pulser Xcell (Bio-Rad Laboratories), with the following settings: 25  $\mu$ FD, 1.25 kV,  $\infty$   $\Omega$ . Stable integrants were selected in media with 50  $\mu$ g/ml of mycophenolic acid (Axxora) and 50  $\mu$ g/ml of xanthine (Alfa Aesar) and cloned by limiting dilution. The correct tagging was confirmed by PCR, using a primer upstream of the plasmid integration site and a primer specific for the HA tag (5'-CGCGTAGTCCGGGACGTCGTACGGGTA-3'), and by an immunofluorescence assay (IFA) using an HA-specific antibody (Sigma, clone 3F10).

For the generation of RH  $\Delta$ rop5 +ROP5A<sub>D</sub> and RH  $\Delta$ rop5 +ROP5B complementation strains, RH *Δhxpprt Δku80 Δrop5::HXGPRT* tachyzoites were transfected by electroporation with linearized pTKO-"ROP5KO" -ROP5A<sub>II-ME49</sub>-His6-3xFlag plasmid [9], or a similarly

generated pTKO -*ROP5*<sub>III-CTG</sub>-*His6-3xFlag* plasmid as described in [9]. In brief, for both strains the complementation allele, *ROP5-His6-3xFlag*, is flanked by homology arms to the  *$\Delta$ rop5::HXGPRT* locus, whereby the transfected population is selected for removal of *HXGPRT* and replacement with the complementation allele in 6-thioxanthine selection medium [177  $\mu$ g/mL of 6-thioxanthine (TRC, cat# T385800) in 4.5 g/liter D-glucose in GlutaMAX DMEM (Gibco), with 1% dialyzed FBS (Omega Scientific, cat#FB-03, lot#463304)]. Post-selection and limiting dilution cloning, *ROP5-His6-3xFlag* complementation strains were assessed by IFA with a mouse anti-Flag primary antibody (Sigma, clone M2) at 1:500 dilution and Alexa Flour 594 goat anti-mouse IgG secondary antibody (Life Technologies) at 1:3000 dilution. Both clones expressed the ROP5-HF in the expected rhoptry organelles by IFA.

For generating the Pru A7  $\Delta$ *hxgp**rt*  $\Delta$ *gra24* strain, Pru A7  $\Delta$ *hxgp**rt* parasites were transfected with a NotI-linearized plasmid expressing a loxP-flanked pyrimethamine selectable cassette (*loxP-DHFR-mCherry-loxP*) (Addgene plasmid #70147, was a gift from David Sibley, Washington University in St. Louis) and a CRISPR-CAS9 construct targeting *GRA24* (*TGME49\_230180*). Transfectants were selected and cloned in medium containing pyrimethamine, and screened for the disruption of *GRA24*. For generating the Pru A7  $\Delta$ *hxgp**rt*  $\Delta$ *gra15*  $\Delta$ *gra24* strain, first the Pru A7  $\Delta$ *hxgp**rt*  $\Delta$ *gra15::HXGPRT* strain [98] was gene-edited with CRISPR-CAS9 targeting *HXGPRT* and selected against its expression with 6-thioxanthine. Then, a Pru A7  $\Delta$ *hxgp**rt*  $\Delta$ *gra15::hxgp**rt*- clone was used to make a Pru A7  $\Delta$ *hxgp**rt*  $\Delta$ *gra15*  $\Delta$ *gra24* double knockout strain using the same method as described above. Finally, the *loxP-DHFR-mCherry-loxP* cassette was removed from both  $\Delta$ *gra24* and  $\Delta$ *gra15*/ $\Delta$ *gra24* strains by transfection with a Cre recombinase parasite-expression plasmid [145], and immediately cloned by limiting dilution. The details of which can be found in a later manuscript by Mukhopadhyay *et al.*

### Immunofluorescence assay

For TGD057 visualization, HFFs were seeded on coverslips with HFF medium in 24-well tissue culture-treated plates. The confluent monolayer HFFs were infected with *T. gondii* and incubated at 37°C, 5% CO<sub>2</sub> overnight. For Irgb6- and p62-PV localization, BMDMs were plated on coverslips with 'BMDM medium' [4.5 g/liter D-glucose in DMEM with GlutaMAX (Gibco), 20% heat-inactivated FBS (Omega Scientific), 1% penicillin-streptomycin (Gibco), 1X non-essential amino acids (Gibco, cat#11140076), 1mM sodium pyruvate (Gibco, cat#11360070)] supplemented with 20% L929 conditioned medium in 24-well tissue culture-treated plates. The BMDMs were treated with 20 ng/ml of IFN $\gamma$  overnight. The cells were then infected with *T. gondii* and incubated at 37°C, 5% CO<sub>2</sub> for 3–4 hours. The samples were fixed with 3% formaldehyde in phosphate buffered saline (PBS) for 20 minutes and blocked with blocking buffer (3% BSA, 5% normal goat serum or fetal bovine serum depending the species of antibody used, 0.2% Triton X-100, 0.1% sodium azide in PBS). To visualize TGD057-HA, RH or RH<sub>Igd057</sub>-HA were stained with rat anti-HA primary antibody (Sigma, clone 3F10) at 1:500 dilution, followed by Alexa Fluor 594 goat anti-rat IgG (Life Technologies) secondary antibody (1:3000 dilution). To visualize p62, infected cells were stained with mouse anti-p62 (anti-SQSTM1) primary monoclonal antibody (Abnova, clone 2C11) at 1:50 or 1:100 dilutions, followed by Alexa Fluor 594 goat anti-mouse IgG (Life Technologies) secondary antibody at 1:3000 dilution. To visualize Irgb6, infected BMDMs were stained with TGTP goat polyclonal primary antibody (Santa Cruz Biotechnology, sc-11079) at 1:100 dilution, followed by Alexa Fluor 594 donkey anti-goat IgG (Life Technologies) at 1:3000 dilution. *T. gondii* PVM was stained with polyclonal rabbit anti-GRA7 primary antibody (gift from John Boothroyd, Stanford University) and Alexa Fluor 488 anti-rabbit IgG (Life Technologies) at 1:3000 dilution.

Host nuclei were visualized with DAPI (Thermo Fisher, cat#62248) at 1:10,000 dilution or Hoechst (Life Technologies, cat# H3075) at 1:3000 dilution.

### Mice and generation of bone marrow-derived macrophages

Six-week-old female *Stat1*<sup>-/-</sup> (colony 012606), *Ifngr*<sup>-/-</sup> (colony 003288), *Nlrp1*<sup>-/-</sup> (colony 021301), *Nlrp3*<sup>-/-</sup> (colony 021302), *Casp1/11*<sup>-/-</sup> (colony 016621), *Il18*<sup>-/-</sup> (colony 004130), and *Il12b*<sup>-/-</sup> (colony 002693) and wildtype C57BL/6J (B6) (colony 000664) mice were purchased from Jackson Laboratories, and all of the C57BL/6 background. C57BL/6 *Asc*<sup>-/-</sup> mice were generous gifts from Vishva Dixit (Genentech). Hind bones from C57BL/6 *Gsdmd*<sup>-/-</sup> mice [146] were generous gifts from Igor Brodsky (University of Pennsylvania). *Irgm1*<sup>-/-</sup> and *Irgm1/m3*<sup>-/-</sup> hind bones were provided from Gregory Taylor (Duke University). *GBP<sup>chr3</sup>*<sup>-/-</sup> hind bone marrow cells were provided by Masahiro Yamamoto (Osaka University). Bone marrow cells were obtained and cultured in BMDM medium supplemented with 20% L929 conditioned medium. After 6–7 days of differentiation, BMDMs were harvested and were 98% pure CD11b<sup>+</sup> CD11c<sup>-</sup> macrophages by FACS. *Asc*<sup>-/-</sup>, *Gsdmd*<sup>-/-</sup>, and *Nlrp3*<sup>-/-</sup> BMDMs were stained with anti-mouse MHC 1 K<sup>b</sup>-PE labeled antibodies (BioLegend, clone AF6-88.5) and they were positive by FACS analysis.

Transnuclear T57 mice [57] were bred in-house under specific pathogen free (SPF) conditions. ‘T-GREAT’ mice were generated by back- and inter-crossing between T57 and IFN $\gamma$ -stop-IRES:eYFP- endogenous poly-A tail reporter mice (GREAT mice) [91], such that breeders obtained from F3 intercrossed mice were homozygous at three alleles: T57 TCR $\alpha$  (*TRAV6-4 TRAJ12* rearrangement), T57 TCR $\beta$  (*TRBV13-1 TRBJ2-7* rearrangement), and the GREAT reporter. T-GREAT mice were then maintained in our SPF facility with no overt fitness defects observed. Genotyping primers were as followed: GREAT allele (FW 5'-CCATGGTGAGCAAGGGCGAGG-3'; RV 5'-TTACTTGTACAGCTCGTCCAT-3'); wildtype *Ifng* allele (FW 5'-CAGGAAGCGGAAAAGGAGTCG-3'; RV 5'-GTCAGTGCAGCTCTGAATGTT-3'); T57 TCR $\alpha$  (*TRAV6-4 TRAJ12* rearrangement: ‘146-alpha’ FW 5'-GATAAGGGATGCTTCAATCTGATGG-3'; ‘108-alpha’ RV 5'-CTTCCTTAGCTCACTTACCAGGGCTTAC-3'); endogenous non-rearranged *TRAV6-4* and *TRAJ12* loci (‘191-alpha’ FW 5'-GAGGCTTACGTTAGTGATCTAAAC-3'; ‘108-alpha’ RV); T57 TCR $\beta$  (*TRBV13-1 TRBJ2-7* rearrangement: ‘91-beta’ FW 5'-CTTGGTCGCGAGATGGGCTCCAG-3'; ‘103-beta’ RV 5'-GTGGAAGCGAGAGATGTGAATCTTAC-3'); endogenous non-rearranged *TCRBV13-1* and *TRBJ2-7* loci (‘142-beta’ FW 5'-GCACTCGGCTCCTCGTGTTAGGTG-3'; ‘103-beta’ RV).

### T cell activation assay

2x10<sup>5</sup> BMDMs cells were plated per well in a 96-well tissue culture-treated plate, in BMDM medium supplemented with 10% L929 conditioned medium. The following day, these BMDMs were infected with *T. gondii* tachyzoites in ‘T cell medium’ [(RPMI 1640 with GlutaMAX (Gibco, cat#61870127), 20% heat-inactivated FBS (Omega Scientific, cat#FB-11, lot#441164), 1% penicillin-streptomycin (Gibco, cat#15140122), 1 mM sodium pyruvate (Gibco, cat#11360070), 10 mM HEPES (Gibco), 1.75  $\mu$ l of  $\beta$ -mercaptoethanol (Gibco, cat#21985023) per 500 mL RPMI 1640 with GlutaMAX]. The infections were performed in triplicates, at MOI 0.6, 0.2, and 0.07. Then, lymph nodes and spleens were obtained from either T57 or T-GREAT transnuclear mice. The lymph node cells and splenocytes were combined and red blood cells were lysed with ammonium chloride-potassium (ACK) lysis buffer. 5x10<sup>5</sup> cells were added into each well of the infected BMDMs (approximately 2 hours post-infection). For IL-1R neutralization, 50  $\mu$ g/mL of anti-mouse IL-1R antibody (BioXCell, clone



JAMA-147) or 50  $\mu$ g/mL of isotype control (BioXCell, cat#BE0091) were added when BMDMs were infected.

### Correction for relative viability between parasites

Confluent monolayer HFFs, seeded in 24-well plates, were infected with 100 and 300 parasites. Plaques were counted 4–6 days after infection. Displayed results are from MOIs with similar viability, the equivalent of  $\sim$ MOI 0.2 was chosen for most assays.

### ELISA

The concentration of cytokines in the 24h and 48h supernatants from the T57 T cell activation assay was measured by ELISA according to the manufacturer's instructions (IFN $\gamma$ : Invitrogen eBioscience, cat#88731477, IL-2: Invitrogen eBioscience, cat#88702477, IL-17A: Invitrogen eBioscience, cat# 88737188, IL-1 $\beta$ : R&D Systems, cat#DY401-05, IL-18: Invitrogen, cat#BMS618-3). The supernatants were analyzed at various dilutions (1:2, 1:20, and 1:200) to obtain values within the linear range of the manufacturer's ELISA standards.

### Flow cytometry

At 18h after T-GREAT T cell activation, samples were harvested for FACS analysis. With preparations all done on ice, cells were washed with 'FACS buffer' [PBS pH 7.4 (Gibco, cat#10010049), 2% heat-inactivated FBS (Omega Scientific)] and blocked with 'blocking buffer' [FACS buffer with 5% normal Syrian hamster serum (Jackson Immunoresearch, cat#007-000-120), 5% normal mouse serum (Jackson Immunoresearch, cat#015-000-120), and anti-mouse CD16/CD32 FcBlock (BD Biosciences, clone 2.4G2) at 1:100 dilution)]. Then, the samples were stained at 1:120 dilution with fluorophore-conjugated anti-mouse monoclonal antibodies against CD8 $\alpha$  PE (eBioscience, clone 53–6.7), CD3 $\epsilon$  APC-eFlour780 (eBioscience, clone 17A2), CD62L eFlour450 (eBioscience, clone MEL-14), and CD69 APC (BioLegend, clone H1.2F3). For analysis of GFP+ Pru A7-infected BMDMs, cells were harvested at 18h, washed and blocked as previously described, and stained at 1:100 dilution with PE-labeled anti-mouse antibodies against CD40 (BioLegend, clone 3/23), CD70 (eBioscience, clone FR70), CD80 (eBioscience, clone 16-10A1), CD86 (eBioscience, clone GL1), CD252 (eBioscience, OX40L clone RM134L), CD274 (eBioscience, PD-L1 clone MIH5), CD275 (eBioscience, ICOSL clone HK5.3), or rat IgG2a kappa isotype control antibodies (eBioscience, clone eBR2a). Tissue culture plates containing the infected BMDMs were placed on ice prior to harvesting and washing as described above. All samples were then stained with propidium iodide (PI) at 1:1000 dilution (Sigma, cat#P4170). Flow cytometry was performed on an LSRII (Becton Dickinson) and analyzed with FlowJo software; PI+ cells were excluded from analysis.

### Statistical analysis and normalization between experiments

For all bar graphs, dots represent values obtained from an individual experiment. Results between parasite strains were often expressed relative to the response elicited by the type II strain (equal 1), or the response to infected knockout macrophages normalized to infected wildtype macrophages (equal 1). All statistical analyses (one-way or two-way ANOVA with Bonferroni's correction, Kruskal-Wallis test with Dunn's correction for non-parametric data in Fig 5, and unpaired two-tailed t-test) were performed with GraphPad Prism version 8.3.0.



## Supporting information

**S1 Fig. Conservation of the TGD057 96–103 peptide epitope and high *TGD057* gene expression between *T. gondii* strains.** (A) Multiple protein alignment of TGD057 (215980) encoded by various *T. gondii* strains; the 96–103 MHC 1 K<sup>b</sup> T57 T cell epitope is highlighted. Dots represent amino acid conservation with TGD057 from the CAST strain. The predicted signal peptide cleavage site and an alternative translational start site [58] is indicated with an arrow. (B) *TGD057* gene expression (TG\_215980) for 29 parasite strains following 20–22 hours post-infection in BMDMs (C57BL/6) is plotted from data previously reported [147]; expression values are in fragments per kilobase of exon model, per million mapped reads (FPKM). (PDF)

**S2 Fig. Negligible amounts of IL-17A, IL-1 $\beta$  and IL-18 are detected in co-cultures of *T. gondii*-infected BMDMs and T57 CD8 T cells.** (A) BMDMs were infected with the indicated parasite strains and IL-17A was measured in the supernatant at 48h post addition of naïve T57 CD8 T cells. Average of 3 experiments + SD are plotted; each dot represents the result from an individual experiment. Statistical analysis was performed with two-way ANOVA with Bonferroni's correction, ns non-significant. (B) BMDMs were infected with RH or Pru strains, and IL-1 $\beta$  or IL-18 was measured in the supernatant at 24h or 48h post addition of naïve T57 CD8 T cells. Plotted is the average + SD of 3 technical replicates. Results obtained at 48 h are representative of two experiments, and a single experiment at 24h was performed. (EPS)

**S3 Fig. TGD057-specific CD8 T cell IL-2 responses to various strains of *T. gondii*.** (A) BMDMs were infected with the indicated clade A RH, RH  $\Delta$ rop5 and  $\Delta$ rop18 strains and IL-2 was measured in the supernatant at 48h post addition of naïve T57 CD8 T cells. Plotted is the average + SD of 3 experiments. Statistical analysis was performed using one-way ANOVA with Bonferroni's correction; \*  $p \leq 0.05$ . (B) BMDMs were infected with *T. gondii* strains—clonal (types I-III), atypical (HG IV-X), and HG XI—representative of various clades and haplogroups. Infected BMDMs were incubated with naïve T57 CD8 T cells for 48 hours and IL-2 concentration in supernatant was measured by ELISA. Each dot represents the result from an individual experiment and the averages + SD of 2–8 experiments per strain are shown. Statistical analysis was performed using one-way ANOVA with Bonferroni's correction; \*  $p \leq 0.05$ . (EPS)

**S4 Fig. Statistical analysis of the T57 IFN $\gamma$  response differences between various *T. gondii* strains.** Statistical analysis of the T57 CD8 T cell IFN $\gamma$  response differences observed to parasite strains from clades A-F, as shown in Fig 5A, was performed using a Kruskal-Wallis non-parametric test with Dunn's correction. Calculated p-values are shown for each strain by strain comparison; p-values  $\leq 0.05$  are highlighted in red and considered significant. As low inducers of IFN $\gamma$ , all clade A strains, as well as TgCatBr5 from clade B, produced statistically significant differences with at least two other parasite strains. (EPS)

**S5 Fig. Surface expression of MHC 1 and several co-stimulatory molecules are not impaired in *T. gondii*-infected *Nlrp3*<sup>-/-</sup> BMDMs.** (A) Gating strategy for flow cytometry analysis of co-stimulatory molecules expressed by infected BMDMs. BMDMs were infected with a GFP-expressing *T. gondii* strain or left uninfected, and later stained with fluorescently labeled marker-specific antibodies. The BMDMs were gated on forward and side scatter, and infected (GFP+) or uninfected (GFP-) live (PI-) BMDMs, shown with indicated frequencies,

were then analyzed for the expression of co-stimulatory molecules. **(B-C)** The surface expression of co-stimulatory molecules and MHC 1 K<sup>b</sup> were analyzed as described in Fig 9C and 9D, and compared **(B)** between infected (GFP+) and uninfected (GFP-) BMDMs, as well as **(C)** between infected *Nlrp3*<sup>-/-</sup> and WT BMDMs (GFP+). Histogram plots are representative of 2–3 experiments.  
(EPS)

## Acknowledgments

We would like to thank Dominique Soldati-Favre (University of Geneva) for the ME49  $\Delta$ *asp5* strain; Igor Brodsky (University of Pennsylvania) for *Gsdmd*<sup>-/-</sup> mouse bones; John Boothroyd (Stanford University) for anti-GRA7 polyclonal rabbit antibodies, ME49  $\Delta$ *myr1*, ME49  $\Delta$ *myr1::MYR1*, and RH  $\Delta$ *rop17* parasite strains; George Yap (Rutgers New Jersey Medical School) for sending the BOF +LC37 strain; Vishva Dixit (Genentech) for sending *Asc*<sup>-/-</sup> mice. We thank April Apostol (UC Merced) for initial help with IFA and visualization of TGD057-HA.

## Author Contributions

**Conceptualization:** Angel K. Kongsomboonvech, Kirk D. C. Jensen.

**Formal analysis:** Angel K. Kongsomboonvech, Felipe Rodriguez, Kirk D. C. Jensen.

**Funding acquisition:** Kirk D. C. Jensen.

**Investigation:** Angel K. Kongsomboonvech, Felipe Rodriguez, Anh L. Diep, Brandon M. Justice, Brayan E. Castellanos, Kirk D. C. Jensen.

**Methodology:** Angel K. Kongsomboonvech, Felipe Rodriguez, Ana Camejo, Debanjan Mukhopadhyay, Gregory A. Taylor, Masahiro Yamamoto, Jeroen P. J. Saeij, Michael L. Reese, Kirk D. C. Jensen.

**Project administration:** Angel K. Kongsomboonvech, Felipe Rodriguez, Kirk D. C. Jensen.

**Resources:** Gregory A. Taylor, Masahiro Yamamoto, Jeroen P. J. Saeij, Michael L. Reese, Kirk D. C. Jensen.

**Supervision:** Kirk D. C. Jensen.

**Validation:** Angel K. Kongsomboonvech, Felipe Rodriguez, Kirk D. C. Jensen.

**Visualization:** Angel K. Kongsomboonvech, Felipe Rodriguez, Kirk D. C. Jensen.

**Writing – original draft:** Angel K. Kongsomboonvech, Kirk D. C. Jensen.

**Writing – review & editing:** Angel K. Kongsomboonvech, Kirk D. C. Jensen.

## References

1. Melo MB, Jensen KDC, Saeij JPJ. Toxoplasma gondii effectors are master regulators of the inflammatory response. Trends in Parasitology. 2011; 27: 487–495. <https://doi.org/10.1016/j.pt.2011.08.001> PMID: 21893432
2. Howard JC, Hunn JP, Steinfeldt T. The IRG protein-based resistance mechanism in mice and its relation to virulence in Toxoplasma gondii. Current Opinion in Microbiology. 2011; 14: 414–421. <https://doi.org/10.1016/j.mib.2011.07.002> PMID: 21783405
3. Reese ML, Shah N, Boothroyd JC, Shah, Boothroyd JC. The Toxoplasma pseudokinase ROP5 is an allosteric inhibitor of the immunity-related GTPases. The Journal of Biological Chemistry. 2014; 289: 27849–27858. <https://doi.org/10.1074/jbc.M114.567057> PMID: 25118287

4. Fleckenstein MC, Reese ML, Konen-Waisman S, Boothroyd JC, Howard JC, Steinfeldt T. A *Toxoplasma gondii* pseudokinase inhibits host IRG resistance proteins. *PLoS Biology*. 2012; 10: e1001358. <https://doi.org/10.1371/journal.pbio.1001358> PMID: 22802726
5. Behnke MS, Fentress SJ, Mashayekhi M, Li LX, Taylor GA, Sibley LD. The Polymorphic Pseudokinase ROP5 Controls Virulence in *Toxoplasma gondii* by Regulating the Active Kinase ROP18. *PLoS Pathogens*. 2012; 8. <https://doi.org/10.1371/journal.ppat.1002992> PMID: 23144612
6. Etheridge RD, Alaganan A, Tang K, Lou HJ, Turk BE, Sibley LD. The *Toxoplasma* pseudokinase ROP5 forms complexes with ROP18 and ROP17 kinases that synergize to control acute virulence in mice. *Cell Host & Microbe*. 2014; 15: 537–550. <https://doi.org/10.1016/j.chom.2014.04.002> PMID: 24832449
7. Fentress SJ, Behnke MS, Dunay IR, Mashayekhi M, Rommereim LM, Fox BA, et al. Phosphorylation of immunity-related GTPases by a *Toxoplasma gondii*-secreted kinase promotes macrophage survival and virulence. *Cell Host & Microbe*. 2010; 8: 484–495. <https://doi.org/10.1016/j.chom.2010.11.005> PMID: 21147463
8. Steinfeldt T, Konen-Waisman S, Tong L, Pawlowski N, Lamkemeyer T, Sibley LD, et al. Phosphorylation of mouse immunity-related GTPase (IRG) resistance proteins is an evasion strategy for virulent *Toxoplasma gondii*. *PLoS Biology*. 2010; 8. <https://doi.org/10.1371/journal.pbio.1000576> PMID: 21203588
9. Reese ML, Zeiner GM, Saeij JPJ, Boothroyd JC, Boyle JP. Polymorphic family of injected pseudokinases is paramount in *Toxoplasma* virulence. *Proceedings of the National Academy of Sciences of the United States of America*. 2011; 108: 9625–9630. <https://doi.org/10.1073/pnas.1015980108> PMID: 21436047
10. Saeij JP, Boyle JP, Collier S, Taylor S, Sibley LD, Brooke-Powell ET, et al. Polymorphic secreted kinases are key virulence factors in toxoplasmosis. *Science*. 2006; 314: 1780–1783. <https://doi.org/10.1126/science.1133690> PMID: 17170306
11. Taylor S, Barragan A, Su C, Fux B, Fentress SJ, Tang K, et al. A secreted serine-threonine kinase determines virulence in the eukaryotic pathogen *Toxoplasma gondii*. *Science*. 2006; 314: 1776–1780. <https://doi.org/10.1126/science.1133643> PMID: 17170305
12. Behnke MS, Khan A, Wootton JC, Dubey JP, Tang K, Sibley LD. Virulence differences in *Toxoplasma* mediated by amplification of a family of polymorphic pseudokinases. *Proceedings of the National Academy of Sciences*. 2011; 108: 9631–9636. <https://doi.org/10.1073/pnas.1015338108> PMID: 21586633
13. Behnke MS, Khan A, Lauron EJ, Jimah JR, Wang Q, Tolia NH, et al. Rhoptry Proteins ROP5 and ROP18 Are Major Murine Virulence Factors in Genetically Divergent South American Strains of *Toxoplasma gondii*. *PLoS genetics*. 2015; 11. <https://doi.org/10.1371/journal.pgen.1005434> PMID: 26291965
14. Kravets E, Degrandi D, Ma Q, Peulen T-O, Klümpers V, Felekyan S, et al. Guanylate binding proteins (GBPs) directly attack *T. gondii* via supramolecular complexes. *eLife*. 2016; 5: 1–30. <https://doi.org/10.7554/eLife.11479> PMID: 26814575
15. Saeij JP, Frickel EM. Exposing *Toxoplasma gondii* hiding inside the vacuole: a role for GBPs, autophagy and host cell death. 2017. <https://doi.org/10.1016/j.mib.2017.10.021> PMID: 29141239
16. Kim BH, Shenoy AR, Kumar P, Bradfield CJ, MacMicking JD. IFN-inducible GTPases in host cell defense. *Cell Host & Microbe*. 2012; 12: 432–444. <https://doi.org/10.1016/j.chom.2012.09.007> PMID: 23084913
17. Yarovinsky F. Innate immunity to *Toxoplasma gondii* infection. *Nature Reviews Immunology*. 2014; 14: 109–121. <https://doi.org/10.1038/nri3598> PMID: 24457485
18. Gigley JP, Bhadra R, Khan IA. CD8 T Cells and *Toxoplasma gondii*: A New Paradigm. *Journal of parasitology research*. 2011; 2011: 243796. <https://doi.org/10.1155/2011/243796> PMID: 21687650
19. Suzuki Y, Oretunua MA, Schreiber RD, Remington JS. Interferon- $\gamma$ : The Major Mediator of Resistance Against *Toxoplasma gondii*. *Science*. 1988; 240: 516–518.
20. Suzuki Y, Remington JS. Dual regulation of resistance against *Toxoplasma gondii* infection by Lyt-2+ and Lyt-1+, L3T4+ T cells in mice. *Journal of Immunology (Baltimore, Md)*. 1988; 140: 3943–3946.
21. Suzuki Y, Remington JS. The effect of anti-IFN- $\gamma$  antibody on the protective effect of Lyt-2+ immune T cells against toxoplasmosis in mice. *J Immunol*. 1990; 144: 1954. PMID: 2106557
22. Gazzinelli R, Xu Y, Hieny S, Cheever A, Sher A. Simultaneous depletion of CD4+ and CD8+ T lymphocytes is required to reactivate chronic infection with *Toxoplasma gondii*. *Journal of Immunology (Baltimore, Md)*. 1992; 149: 175–180.

23. Suzuki Y, Conley FK, Remington JS. Importance of endogenous IFN-gamma for prevention of toxoplasmic encephalitis in mice. *Journal of Immunology* (Baltimore, Md: 1950). 1989; 143: 2045–2050.
24. Gigley JP, Fox BA, Bzik DJ. Cell-mediated immunity to *Toxoplasma gondii* develops primarily by local Th1 host immune responses in the absence of parasite replication. *Journal of Immunology* (Baltimore, Md: 1950). 2009; 182: 1069–1078. <https://doi.org/10.4049/jimmunol.182.2.1069> PMID: 19124750
25. Gazzinelli RT, Hakim FT, Hieny S, Shearer GM, Sher A. Synergistic role of CD4+ and CD8+ T lymphocytes in IFN-gamma production and protective immunity induced by an attenuated *Toxoplasma gondii* vaccine. *Journal of Immunology* (Baltimore, Md: 1950). 1991; 146: 286–292.
26. Jensen KDC, Camejo A, Melo MB, Cordeiro C, Julien L, Grotenbreg GM, et al. *Toxoplasma gondii* superinfection and virulence during secondary infection correlate with the exact ROP5/ROP18 allelic combination. *mBio*. 2015; 6. <https://doi.org/10.1128/mBio.02280-14> PMID: 25714710
27. Sacks DL. Vaccines against tropical parasitic diseases: a persisting answer to a persisting problem. *Nature Immunology*. 2014; 15: 403–405. <https://doi.org/10.1038/ni.2853> PMID: 24747701
28. Christiaansen A, Varga SM, Spencer JV. Viral manipulation of the host immune response. *Current Opinion in Immunology*. 2015; 36: 54–60. <https://doi.org/10.1016/j.coi.2015.06.012> PMID: 26177523
29. Gubbels MJ, Striepen B, Shastri N, Turkoz M, Robey EA. Class I major histocompatibility complex presentation of antigens that escape from the parasitophorous vacuole of *Toxoplasma gondii*. *Infection and Immunity*. 2005; 73: 703–711. <https://doi.org/10.1128/IAI.73.2.703-711.2005> PMID: 15664908
30. Dzierszynski F, Pepper M, Stumhofer JS, LaRosa DF, Wilson EH, Turka LA, et al. Presentation of *Toxoplasma gondii* antigens via the endogenous major histocompatibility complex class I pathway in nonprofessional and professional antigen-presenting cells. *Infection and Immunity*. 2007; 75: 5200–5209. <https://doi.org/10.1128/IAI.00954-07> PMID: 17846116
31. Blanchard N, Gonzalez F, Schaeffer M, Joncker NT, Cheng T, Shastri AJ, et al. Immunodominant, protective response to the parasite *Toxoplasma gondii* requires antigen processing in the endoplasmic reticulum. *Nature Immunology*. 2008; 9: 937–944. <https://doi.org/10.1038/ni.1629> PMID: 18587399
32. Feliu V, Vasseur V, Grover HS, Chu HH, Brown MJ, Wang J, et al. Location of the CD8 T cell epitope within the antigenic precursor determines immunogenicity and protection against the *Toxoplasma gondii* parasite. *PLoS Pathogens*. 2013; 9: e1003449. <https://doi.org/10.1371/journal.ppat.1003449> PMID: 23818852
33. Dupont CD, Christian DA, Selleck EM, Pepper M, Leney-Greene M, Pritchard GH, et al. Parasite fate and involvement of infected cells in the induction of CD4+ and CD8+ T cell responses to *Toxoplasma gondii*. *PLoS Pathogens*. 2014; 10: e1004047. <https://doi.org/10.1371/journal.ppat.1004047> PMID: 24722202
34. Goldszmid RS, Coppens I, Lev A, Caspar P, Mellman I, Sher A. Host ER-parasitophorous vacuole interaction provides a route of entry for antigen cross-presentation in *Toxoplasma gondii*-infected dendritic cells. *The Journal of Experimental Medicine*. 2009; 206: 399–410. <https://doi.org/10.1084/jem.20082108> PMID: 19153244
35. Grover HS, Chu HH, Kelly FD, Yang SJ, Reese ML, Blanchard N, et al. Impact of regulated secretion on antiparasitic CD8 T cell responses. *Cell Reports*. 2014; 7: 1716–1728. <https://doi.org/10.1016/j.celrep.2014.04.031> PMID: 24857659
36. Bertholet S, Goldszmid R, Morrot A, Debrabant A, Afrin F, Collazo-Custodio C, et al. Leishmania Antigens Are Presented to CD8+ T Cells by a Transporter Associated with Antigen Processing-Independent Pathway In Vitro and In Vivo. *J Immunol*. 2006; 177: 3525. <https://doi.org/10.4049/jimmunol.177.6.3525> PMID: 16951311
37. Sinai AP, Webster P, Joiner KA. Association of host cell endoplasmic reticulum and mitochondria with the *Toxoplasma gondii* parasitophorous vacuole membrane: a high affinity interaction. *Journal of Cell Science*. 1997; 110: 2117–2128. PMID: 9378762
38. Coppens I. How *Toxoplasma* and malaria parasites defy first, then exploit host autophagic and endocytic pathways for growth. 2017; 32–39.
39. Jensen KDC. Antigen Presentation of Vacuolated Apicomplexans—Two Gateways to a Vaccine Antigen. *Trends in Parasitology*. 2016; 32: 88–90. <https://doi.org/10.1016/j.pt.2015.12.011> PMID: 26733404
40. Fox BA, Butler KL, Guevara RB, Bzik DJ. Cancer therapy in a microbial bottle: Uncorking the novel biology of the protozoan *Toxoplasma gondii*. *PLOS Pathogens*. 2017; 13: e1006523. <https://doi.org/10.1371/journal.ppat.1006523> PMID: 28910406
41. Lopez J, Bittame A, Massera C, Vasseur V, Effantin G, Valat A, et al. Intravacuolar Membranes Regulate CD8 T Cell Recognition of Membrane-Bound *Toxoplasma gondii* Protective Antigen. *Cell Reports*. 2015; 13: 2273–2286. <https://doi.org/10.1016/j.celrep.2015.11.001> PMID: 26628378

42. Buillon C, Guerrero NA, Cebrian I, Blanié S, Lopez J, Bassot E, et al. MHC I presentation of *Toxoplasma gondii* immunodominant antigen does not require Sec22b and is regulated by antigen orientation at the vacuole membrane. *European Journal of Immunology*. 2017; 47: 1160–1170. <https://doi.org/10.1002/eji.201646859> PMID: 28508576
43. Cebrian I, Visentin G, Blanchard N, Jouve M, Bobard A, Moita C, et al. Sec22b regulates phagosomal maturation and antigen crosspresentation by dendritic cells. *Cell*. 2011; 147: 1355–1368. <https://doi.org/10.1016/j.cell.2011.11.021> PMID: 22153078
44. Lee Y, Sasai M, Ma JS, Sakaguchi N, Ohshima J, Bando H. p62 plays a specific role in interferon- $\gamma$ -induced presentation of a *Toxoplasma* vacuolar antigen. *Cell Rep*. 2015; 13. <https://doi.org/10.1016/j.celrep.2015.09.005> PMID: 26440898
45. Rommereim LM, Fox BA, Butler KL, Cantillana V, Taylor GA, Bzik DJ. Rhopty and Dense Granule Secreted Effectors Regulate CD8+ T Cell Recognition of *Toxoplasma gondii* Infected Host Cells. *Frontiers in Immunology*. 2019; 10: 2104. <https://doi.org/10.3389/fimmu.2019.02104> PMID: 31555296
46. Villegas EN, Elloso MM, Reichmann G, Peach R, Hunter CA. Role of CD28 in the Generation of Effector and Memory Responses Required for Resistance to *Toxoplasma gondii*. *The Journal of Immunology*. 1999; 163: 3344–3353. PMID: 10477604
47. Villegas EN, Lieberman LA, Mason N, Blass SL, Zediak VP, Peach R, et al. A Role for Inducible Costimulator Protein in the CD28-Independent Mechanism of Resistance to *Toxoplasma gondii*. *The Journal of Immunology*. 2002; 169: 937–943. <https://doi.org/10.4049/jimmunol.169.2.937> PMID: 12097399
48. Wilson DC, Matthews S, Yap GS. IL-12 Signaling Drives CD8+ T Cell IFN- $\gamma$  Production and Differentiation of KLRG1+ Effector Subpopulations during *Toxoplasma gondii* Infection. *The Journal of Immunology*. 2008; 180: 5935–5945. <https://doi.org/10.4049/jimmunol.180.9.5935> PMID: 18424713
49. Wilson DC, Grotenbreg GM, Liu K, Zhao Y, Frickel EM, Gubbels MJ, et al. Differential regulation of effector- and central-memory responses to *Toxoplasma gondii* Infection by IL-12 revealed by tracking of Tgd057-specific CD8+ T cells. *PLoS Pathogens*. 2010; 6: e1000815. <https://doi.org/10.1371/journal.ppat.1000815> PMID: 20333242
50. Chang HR, Grau GE, Pechère JC. Role of TNF and IL-1 in infections with *Toxoplasma gondii*. *Immunology*. 1990; 69: 33–37. PMID: 2107144
51. Hunter CA, Chizzonite R, Remington JS. IL-1 beta is required for IL-12 to induce production of IFN- $\gamma$  by NK cells. A role for IL-1 beta in the T cell-independent mechanism of resistance against intracellular pathogens. *The Journal of Immunology*. 1995; 155: 4347–4354. PMID: 7594594
52. Gorfou G, Cirelli KM, Melo MB, Mayer-Barber K, Crown D, Koller BH, et al. Dual Role for Inflammasome Sensors NLRP1 and NLRP3 in Murine Resistance to *Toxoplasma gondii*. *mBio*. 2014; 5: e01117–13. <https://doi.org/10.1128/mBio.01117-13> PMID: 24549849
53. Ewald SE, Chavarria-Smith J, Boothroyd JC. NLRP1 Is an Inflammasome Sensor for *Toxoplasma gondii*. Adams JH, editor. *Infection and Immunity*. 2014; 82: 460–468. <https://doi.org/10.1128/IAI.01170-13> PMID: 24218483
54. Pandori WJ, Lima TS, Mallya S, Kao TH, Gov L, Lodoen MB. *Toxoplasma gondii* activates a Syk-CARD9-NF- $\kappa$ B signaling axis and gasdermin D-independent release of IL-1 $\beta$  during infection of primary human monocytes. *PLoS Pathogens*. 2019; 15: 1–24. <https://doi.org/10.1371/journal.ppat.1007923> PMID: 31449558
55. Vossenkämper A, Struck D, Alvarado-Esquivel C, Went T, Takeda K, Akira S, et al. Both IL-12 and IL-18 contribute to small intestinal Th1-type immunopathology following oral infection with *Toxoplasma gondii*, but IL-12 is dominant over IL-18 in parasite control. *European Journal of Immunology*. 2004; 34: 3197–3207. <https://doi.org/10.1002/eji.200424993> PMID: 15368276
56. López-Yglesias AH, Camanzo E, Martin AT, Araujo AM, Yarovinsky F. TLR11-independent inflammasome activation is critical for CD4+ T cell-derived IFN- $\gamma$  production and host resistance to *Toxoplasma gondii*. *PLoS Pathogens*. 2019; 15: 1–20. <https://doi.org/10.1371/journal.ppat.1007872> PMID: 31194844
57. Kirak O, Frickel EM, Grotenbreg GM, Suh H, Jaenisch R, Ploegh HL. Transnuclear mice with predefined T cell receptor specificities against *Toxoplasma gondii* obtained via SCNT. *Science*. 2010; 328: 243–248. <https://doi.org/10.1126/science.1178590> PMID: 20378817
58. Wan K; Ajioka J. Molecular Characterization of tgd057, a Novel Gene from *Toxoplasma gondii*. *Journal of Biochemistry and Molecular Biology*. 2004. <https://doi.org/10.5483/BMBRep.2004.37.4.474> PMID: 15469736
59. Sidik SM, Huet D, Ganesan SM, Carruthers VB, Niles JC, Lourido S, et al. A Genome-wide CRISPR Screen in *Toxoplasma* Identifies Essential Apicomplexan Genes. *Cell*. 2016; 166: 1423–1430. <https://doi.org/10.1016/j.cell.2016.08.019> PMID: 27594426



60. Northrop JP, Ho SN, Chen L, Thomas DJ, Timmerman LA, Nolan GP, et al. NF-AT components define a family of transcription factors targeted in T-cell activation. *Nature*. 1994; 369: 497–502. <https://doi.org/10.1038/369497a0> PMID: 8202141
61. Tsitsiklis A, Bangs DJ, Robey EA. CD8+ T Cell Responses to *Toxoplasma gondii*: Lessons from a Successful Parasite. *Trends in Parasitology*. 2019; 35: 887–898. <https://doi.org/10.1016/j.pt.2019.08.005> PMID: 31601477
62. Crook OM, Mulvey CM, Kirk PDW, Lilley KS, Gatto L. A Bayesian mixture modelling approach for spatial proteomics. *PLoS Computational Biology*. 2018; 14: 1–29. <https://doi.org/10.1371/journal.pcbi.1006516> PMID: 30481170
63. Hammoudi PM, Jacot D, Mueller C, Cristina MD, Dogga SK, Marq JB, et al. Fundamental Roles of the Golgi-Associated *Toxoplasma* Aspartyl Protease, ASP5, at the Host-Parasite Interface. *PLoS Pathogens*. 2015; 11.
64. Coffey MJ, Sleebs BE, Uboldi AD, Garnham A, Franco M, Marino ND, et al. An aspartyl protease defines a novel pathway for export of *Toxoplasma* proteins into the host cell. *eLife*. 2015; 4: 1–34. <https://elifesciences.org/lookup/doi/10.7554/eLife.10809.001>
65. Franco M, Panas MW, Marino ND, Lee M-CW, Buchholz KR, Kelly FD, et al. A Novel Secreted Protein, MYR1, Is Central to *Toxoplasma*'s Manipulation of Host Cells. *mBio*. 2016; 7: e02231–15. <https://doi.org/10.1128/mBio.02231-15> PMID: 26838724
66. Boddey JA, Cowman AF. Plasmodium Nesting: Remaking the Erythrocyte from the Inside Out. *Annual Review of Microbiology*. 2013; 67: 243–269. <https://doi.org/10.1146/annurev-micro-092412-155730> PMID: 23808341
67. Russo I, Babbitt S, Muralidharan V, Butler T, Oksman A, Goldberg DE. Plasmepsin V licenses Plasmodium proteins for export into the host erythrocyte. *Nature*. 2010; 463: 632–636. <https://doi.org/10.1038/nature08726> PMID: 20130644
68. Rastogi S, Cygan AM, Boothroyd JC. Translocation of effector proteins into host cells by *Toxoplasma gondii*. *Current Opinion in Microbiology*. 2019; 52: 130–138. <https://doi.org/10.1016/j.mib.2019.07.002> PMID: 31446366
69. Curt-vaesano A, Braun L, Ranquet C, Hakimi M, Bougdour A. The aspartyl protease TgASP5 mediates the export of the *Toxoplasma* GRA16 and GRA24 effectors into host cells. *Cell Microbiol*. 2016; 18: 151–167. <https://doi.org/10.1111/cmi.12498> PMID: 26270241
70. Braun L, Brenier-Pinchart M-P, Hammoudi P-M, Cannella D, Kieffer-Jaquinod S, Vollaire J, et al. The *Toxoplasma* effector TEEGR promotes parasite persistence by modulating NF- $\kappa$ B signalling via EZH2. *Nature Microbiology*. 2019; 4: 1208–1220. <https://doi.org/10.1038/s41564-019-0431-8> PMID: 31036909
71. Panas MW, Naor A, Cygan AM, Boothroyd JC. *Toxoplasma* Controls Host Cyclin E Expression through the Use of a Novel MYR1-Dependent Effector Protein, HCE1. Weiss LM, editor. *mBio*. 2019; 10. <https://doi.org/10.1128/mBio.00674-19> PMID: 31040242
72. Gregg B, Dzierszinski F, Tait E, Jordan KA, Hunter CA, Roos DS. Subcellular antigen location influences T-Cell activation during acute infection with *Toxoplasma gondii*. *PLoS One*. 2011; 6: 1–7. <https://doi.org/10.1371/journal.pone.0022936> PMID: 21829561
73. Yamamoto M, Okuyama M, Ma JS, Kimura T, Kamiyama N, Saiga H, et al. A cluster of interferon-gamma-inducible p65 GTPases plays a critical role in host defense against *Toxoplasma gondii*. *Immunity*. 2012; 37: 302–313. <https://doi.org/10.1016/j.immuni.2012.06.009> PMID: 22795875
74. Bekpen C, Hunn JP, Rohde C, Parvanova I, Guethlein L, Dunn DM, et al. The interferon-inducible p47 (IRG) GTPases in vertebrates: loss of the cell autonomous resistance mechanism in the human lineage. *Genome Biology*. 2005; 6.
75. Martens S, Parvanova I, Zerrahn J, Griffiths G, Schell G, Reichmann G, et al. Disruption of *Toxoplasma gondii* parasitophorous vacuoles by the mouse p47-resistance GTPases. *PLoS Pathogens*. 2005; 1: e24. <https://doi.org/10.1371/journal.ppat.0010024> PMID: 16304607
76. Zhao Y, Ferguson DJ, Wilson DC, Howard JC, Sibley LD, Yap GS. Virulent *Toxoplasma gondii* evade immunity-related GTPase-mediated parasite vacuole disruption within primed macrophages. *Journal of Immunology (Baltimore, Md: 1950)*. 2009; 182: 3775–3781. <https://doi.org/10.4049/jimmunol.0804190> PMID: 19265156
77. Pawlowski N, Khaminets A, Hunn JP, Papic N, Schmidt A, Uthaiha RC, et al. The activation mechanism of Irga6, an interferon-inducible GTPase contributing to mouse resistance against *Toxoplasma gondii*. *BMC Biology*. 2011; 9: 7. <https://doi.org/10.1186/1741-7007-9-7> PMID: 21276251
78. Haldar AK, Saka HA, Piro AS, Dunn JD, Henry SC, Taylor GA, et al. IRG and GBP host resistance factors target aberrant, “non-self” vacuoles characterized by the missing of “self” IRGM proteins. *PLoS Pathogens*. 2013; 9: e1003414. <https://doi.org/10.1371/journal.ppat.1003414> PMID: 23785284



79. Maric-Biresev J, Hunn JP, Krut O, Helms JB, Martens S, Howard JC. Loss of the interferon-gamma-inducible regulatory immunity-related GTPase (IRG), *Irgm1*, causes activation of effector IRG proteins on lysosomes, damaging lysosomal function and predicting the dramatic susceptibility of *Irgm1*-deficient mice to infection. *BMC Biology*. 2016; 14: 33–34. <https://doi.org/10.1186/s12915-016-0255-4> PMID: 27098192
80. Hunn JP, Koenen-Waisman S, Papic N, Schroeder N, Pawlowski N, Lange R, et al. Regulatory interactions between IRG resistance GTPases in the cellular response to *Toxoplasma gondii*. *EMBO*. 2008; 27: 2495–2509. <https://doi.org/10.1038/emboj.2008.176> PMID: 18772884
81. Niedelman W, Gold DA, Rosowski EE, Sprockholt JK, Lim D, Farid Arenas A, et al. The Rhoptyr Proteins ROP18 and ROP5 Mediate *Toxoplasma gondii* Evasion of the Murine, But Not the Human, Interferon-Gamma Response. Soldati-Favre D, editor. *PLoS Pathogens*. 2012; 8: e1002784. <https://doi.org/10.1371/journal.ppat.1002784> PMID: 22761577
82. Henry SC, Daniell XG, Burroughs AR, Indaram M, Howell DN, Coers J, et al. Balance of *Irgm* protein activities determines IFN-gamma-induced host defense. *Journal of Leukocyte Biology*. 2009; 85: 877–885. <https://doi.org/10.1189/jlb.1008599> PMID: 19176402
83. Taylor GA, Collazo CM, Yap GS, Nguyen K, Gregorio TA, Taylor LS, et al. Pathogen-specific loss of host resistance in mice lacking the IFN-gamma-inducible gene *IGTP*. *Proceedings of the National Academy of Sciences of the United States of America*. 2000; 97: 751–755. <https://doi.org/10.1073/pnas.97.2.751> PMID: 10639151
84. Selleck EM, Fentress SJ, Beatty WL, Grandi D, Pfeffer K, V HW 4th, et al. Guanylate-binding protein 1 (*Gbp1*) contributes to cell-autonomous immunity against *Toxoplasma gondii*. *PLoS Pathogens*. 2013; 9: e1003320. <https://doi.org/10.1371/journal.ppat.1003320> PMID: 23633952
85. Reese ML, Boothroyd JC. A conserved non-canonical motif in the pseudoactive site of the ROP5 pseudokinase domain mediates its effect on *Toxoplasma* virulence. *The Journal of Biological Chemistry*. 2011; 286: 29366–29375. <https://doi.org/10.1074/jbc.M111.253435> PMID: 21708941
86. Taylor GA, Feng CG, Sher A. Control of IFN-g-mediated host resistance to intracellular pathogens by immunity-related GTPases (p47 GTPases). *Microbes and Infection*. 2007; 9: 1644–1651. <https://doi.org/10.1016/j.micinf.2007.09.004> PMID: 18023232
87. Virreira Winter S, Niedelman W, Jensen KD, Rosowski EE, Julien L, Spooner E. Determinants of GBP recruitment to *Toxoplasma gondii* vacuoles and the parasitic factors that control it. *PLoS One*. 2011; 6. <https://doi.org/10.1371/journal.pone.0024434> PMID: 21931713
88. Liesenfeld O, Parvanova I, Zerrahn J, Han S-J, Heinrich F, Muñoz M, et al. The IFN- $\gamma$ -Inducible GTPase, *Irga6*, Protects Mice against *Toxoplasma gondii* but Not against *Plasmodium berghei* and Some Other Intracellular Pathogens. *PLoS One*. 2011; 6: 1–12. <https://doi.org/10.1371/journal.pone.0020568> PMID: 21698150
89. Lee Y, Yamada H, Pradipta A, Ma JS, Okamoto M, Nagaoka H, et al. Initial phospholipid-dependent *Irgb6* targeting to *Toxoplasma gondii* vacuoles mediates host defense. *Life Science Alliance*. 2020; 3. <https://doi.org/10.26508/lsa.201900549> PMID: 31852733
90. Lorenzi H, Khan A, Behnke MS, Namasivayam S, Swapna LS, Hadjithomas M, et al. Local admixture of amplified and diversified secreted pathogenesis determinants shapes mosaic *Toxoplasma gondii* genomes. *Nature Communications*. 2016; 7: 10147. <https://doi.org/10.1038/ncomms10147> PMID: 26738725
91. Reinhardt RL, Liang H-E, Bao K, Price AE, Mohrs M, Kelly BL, et al. A Novel Model for IFN- $\gamma$ -Mediated Autoinflammatory Syndromes. *The Journal of Immunology*. 2015; 194: 2358–2368. <https://doi.org/10.4049/jimmunol.1401992> PMID: 25637019
92. Cebrián M, Yagüe E, Rincón M, López-Botet M, de Landázuri MO, Sánchez-Madrid F. Triggering of T cell proliferation through AIM, an activation inducer molecule expressed on activated human lymphocytes. *The Journal of Experimental Medicine*. 1988; 168: 1621–1637. <https://doi.org/10.1084/jem.168.5.1621> PMID: 2903209
93. Scharton-Kersten TM, Wynn TA, Denkers EY, Bala S, Grunvald E, Hieny S, et al. In the absence of endogenous IFN-gamma, mice develop unimpaired IL-12 responses to *Toxoplasma gondii* while failing to control acute infection. *J Immunol*. 1996; 157: 4045. PMID: 8892638
94. Ely KH, Kasper LH, Khan IA. Augmentation of the CD8+ T Cell Response by IFN- $\gamma$  in IL-12-Deficient Mice During *Toxoplasma gondii* Infection. *The Journal of Immunology*. 1999; 162: 5449–5454. PMID: 10228024
95. Shaw MH, Boyartchuk V, Wong S, Karaghiosoff M, Ragimbeau J, Pellegrini S, et al. A natural mutation in the *Tyk2* pseudokinase domain underlies altered susceptibility of B10.Q/J mice to infection and autoimmunity. *Proceedings of the National Academy of Sciences of the United States of America*. 2003; 100: 11594–11599. <https://doi.org/10.1073/pnas.1930781100> PMID: 14500783

96. Robben PM, Mordue DG, Truscott SM, Takeda K, Akira S, Sibley LD. Production of IL-12 by Macrophages Infected with *Toxoplasma gondii* Depends on the Parasite Genotype. *The Journal of Immunology*. 2004; 172: 3686–3694. <https://doi.org/10.4049/jimmunol.172.6.3686> PMID: 15004172
97. Kim L, Butcher BA, Lee CW, Uematsu S, Akira S, Denkers EY. *Toxoplasma gondii* Genotype Determines MyD88-Dependent Signaling in Infected Macrophages. *The Journal of Immunology*. 2006; 177: 2584–2591. <https://doi.org/10.4049/jimmunol.177.4.2584> PMID: 16888020
98. Rosowski EE, Lu D, Julien L, Rodda L, Gaiser RA, Jensen KD, et al. Strain-specific activation of the NF- $\kappa$ B pathway by GRA15, a novel *Toxoplasma gondii* dense granule protein. *The Journal of Experimental Medicine*. 2011; 208: 195–212. <https://doi.org/10.1084/jem.20100717> PMID: 21199955
99. Butcher BA, Fox BA, Rommereim LM, Kim SG, Maurer KJ, Yarovinsky F, et al. *Toxoplasma gondii* Rho GTPase Kinase ROP16 Activates STAT3 and STAT6 Resulting in Cytokine Inhibition and Arginase-1-Dependent Growth Control. *PLOS Pathogens*. 2011; 7. <https://doi.org/10.1371/journal.ppat.1002236> PMID: 21931552
100. Jensen KD, Wang Y, Wojno ED, Shastri AJ, Hu K, Cornel L, et al. *Toxoplasma* polymorphic effectors determine macrophage polarization and intestinal inflammation. *Cell Host & Microbe*. 2011; 9: 472–483. <https://doi.org/10.1016/j.chom.2011.04.015> PMID: 21669396
101. Braun L, Brenier-Pinchart M-P, Yogavel M, Curt-Varesano A, Curt-Bertini R-L, Hussain T, et al. A *Toxoplasma* dense granule protein, GRA24, modulates the early immune response to infection by promoting a direct and sustained host p38 MAPK activation. *J Exp Med*. 2013; 210: 2071. <https://doi.org/10.1084/jem.20130103> PMID: 24043761
102. Sangaré LO, Yang N, Konstantinou EK, Lu D, Mukhopadhyay D, Young LH, et al. *Toxoplasma* GRA15 Activates the NF- $\kappa$ B Pathway through Interactions with TNF Receptor-Associated Factors. Weiss LM, editor. *mBio*. 2019; 10: e00808–19. <https://doi.org/10.1128/mBio.00808-19> PMID: 31311877
103. Melo MB, Nguyen QP, Cordeiro C, Hassan MA, Yang N, McKell R, et al. Transcriptional Analysis of Murine Macrophages Infected with Different *Toxoplasma* Strains Identifies Novel Regulation of Host Signaling Pathways. *PLOS Pathogens*. 2013; 9: e1003779. <https://doi.org/10.1371/journal.ppat.1003779> PMID: 24367253
104. Saeij JPJ, Collier S, Boyle JP, Jerome ME, White MW, Boothroyd JC. *Toxoplasma* co-opts host gene expression by injection of a polymorphic kinase homologue. *Nature*. 2007; 445: 324–327. <https://doi.org/10.1038/nature05395> PMID: 17183270
105. Yamamoto M, Standley DM, Takashima S, Saiga H, Okuyama M, Kayama H, et al. A single polymorphic amino acid on *Toxoplasma gondii* kinase ROP16 determines the direct and strain-specific activation of Stat3. *The Journal of Experimental Medicine*. 2009; 206: 2747–2760. <https://doi.org/10.1084/jem.20091703> PMID: 19901082
106. Ong YC, Reese ML, Boothroyd JC. *Toxoplasma* rho GTPase protein 16 (ROP16) subverts host function by direct tyrosine phosphorylation of STAT6. *The Journal of Biological Chemistry*. 2010; 285: 28731–28740. <https://doi.org/10.1074/jbc.M110.112359> PMID: 20624917
107. Jensen KD, Hu K, Whitmarsh RJ, Hassan MA, Julien L, Lu D, et al. *Toxoplasma gondii* rho GTPase kinase promotes host resistance to oral infection and intestinal inflammation only in the context of the dense granule protein GRA15. *Infection and Immunity*. 2013; 81: 2156–2167. <https://doi.org/10.1128/IAI.01185-12> PMID: 23545295
108. Cirelli KM, Gofu G, Hassan MA, Printz M, Crown D, Leppla SH, et al. Inflammasome Sensor NLRP1 Controls Rat Macrophage Susceptibility to *Toxoplasma gondii*. *PLoS Pathogens*. 2014. <https://doi.org/10.1371/journal.ppat.1003927> PMID: 24626226
109. Afonina IS, Müller C, Martin SJ, Beyaert R. Proteolytic Processing of Interleukin-1 Family Cytokines: Variations on a Common Theme. *Immunity*. 2015; 42: 991–1004. <https://doi.org/10.1016/j.immuni.2015.06.003> PMID: 26084020
110. Evavold CL, Kagan JC. How Inflammasomes Inform Adaptive Immunity. *Journal of Molecular Biology*. 2018; 430: 217–237. <https://doi.org/10.1016/j.jmb.2017.09.019> PMID: 28987733
111. Broz P, Dixit VM. Inflammasomes: mechanism of assembly, regulation and signalling. *Nature Reviews Immunology*. 2016; 16: 407–420. <https://doi.org/10.1038/nri.2016.58> PMID: 27291964
112. Kayagaki N, Stowe IB, Lee BL, O'Rourke K, Anderson K, Warming S, et al. Caspase-11 cleaves gasdermin D for non-canonical inflammasome signalling. *Nature*. 2015; 526: 666–671. <https://doi.org/10.1038/nature15541> PMID: 26375259
113. Shi J, Zhao Y, Wang K, Shi X, Wang Y, Huang H, et al. Cleavage of GSDMD by inflammatory caspases determines pyroptotic cell death. *Nature*. 2015; 526: 660. <https://doi.org/10.1038/nature15514> PMID: 26375003

114. Ding J, Wang K, Liu W, She Y, Sun Q, Shi J, et al. Pore-forming activity and structural autoinhibition of the gasdermin family. *Nature*. 2016; 535: 111–116. <https://doi.org/10.1038/nature18590> PMID: [27281216](https://pubmed.ncbi.nlm.nih.gov/27281216/)
115. Liu X, Zhang Z, Ruan J, Pan Y, Magupalli VG, Wu H, et al. Inflammasome-activated gasdermin D causes pyroptosis by forming membrane pores. *Nature*. 2016;535. <https://doi.org/10.1038/nature18629> PMID: [27383986](https://pubmed.ncbi.nlm.nih.gov/27383986/)
116. He W, Wan H, Hu L, Chen P, Wang X, Huang Z, et al. Gasdermin D is an executor of pyroptosis and required for interleukin-1 $\beta$  secretion. *Cell Research*. 2015; 25: 1285–1298. <https://doi.org/10.1038/cr.2015.139> PMID: [26611636](https://pubmed.ncbi.nlm.nih.gov/26611636/)
117. Evavold CL, Ruan J, Tan Y, Xia S, Wu H, Kagan JC. The Pore-Forming Protein Gasdermin D Regulates Interleukin-1 Secretion from Living Macrophages. *Immunity*. 2018; 48: 35–44.e6. <https://doi.org/10.1016/j.immuni.2017.11.013> PMID: [29195811](https://pubmed.ncbi.nlm.nih.gov/29195811/)
118. Salerno F, Guislain A, Freen-Van Heeren JJ, Nicolet BP, Young HA, Wolkers MC. Critical role of post-transcriptional regulation for IFN- $\gamma$  in tumor-infiltrating T cells. *Oncoimmunology*. 2019; 8: e1532762. <https://doi.org/10.1080/2162402X.2018.1532762> PMID: [30713785](https://pubmed.ncbi.nlm.nih.gov/30713785/)
119. Villarino AV, Katzman SD, Gallo E, Miller O, Jiang S, McManus MT, et al. Posttranscriptional Silencing of Effector Cytokine mRNA Underlies the Anergic Phenotype of Self-Reactive T Cells. *Immunity*. 2011; 34: 50–60. <https://doi.org/10.1016/j.immuni.2010.12.014> PMID: [21236706](https://pubmed.ncbi.nlm.nih.gov/21236706/)
120. Morgado P, Sudarshana DM, Gov L, Harker KS, Lam T, Casali P, et al. Type II *Toxoplasma gondii* induction of CD40 on infected macrophages enhances interleukin-12 responses. *Infection and Immunity*. 2014;82. <https://doi.org/10.1128/IAI.01615-14> PMID: [25024369](https://pubmed.ncbi.nlm.nih.gov/25024369/)
121. Meissner TB, Li A, Biswas A, Lee K-H, Liu Y-J, Bayir E, et al. NLR family member NLRC5 is a transcriptional regulator of MHC class I genes. *Proceedings of the National Academy of Sciences of the United States of America*. 2010; 107: 13794–13799. <https://doi.org/10.1073/pnas.1008684107> PMID: [20639463](https://pubmed.ncbi.nlm.nih.gov/20639463/)
122. Koch CP, Perna AM, Pillong M, Todoroff NK, Wrede P, Folkers G, et al. Scrutinizing MHC-I Binding Peptides and Their Limits of Variation. *PLoS Computational Biology*. 2013; 9: 1–9. <https://doi.org/10.1371/journal.pcbi.1003088> PMID: [23754940](https://pubmed.ncbi.nlm.nih.gov/23754940/)
123. Coffey MJ, Dagley LF, Seizova S, Kapp EA, Infusini G, Roos DS, et al. Aspartyl Protease 5 Matures Dense Granule Proteins That Reside at the Host-Parasite Interface in *Toxoplasma gondii*. Sibley LD, editor. *mBio*. 2018; 9. <https://doi.org/10.1128/mBio.01796-18> PMID: [30377279](https://pubmed.ncbi.nlm.nih.gov/30377279/)
124. Gay G, Braun L, Brenier-Pinchart M-P, Voltaire J, Josserand V, Bertini R-L, et al. *Toxoplasma gondii* TgIST co-opts host chromatin repressors dampening STAT1-dependent gene regulation and IFN- $\gamma$ -mediated host defenses. *The Journal of Experimental Medicine*. 2016; 213. <https://doi.org/10.1084/jem.20160340> PMID: [27503074](https://pubmed.ncbi.nlm.nih.gov/27503074/)
125. Wang Y, Cirelli KM, Barros PDC, Sangaré LO, Butty V, Hassan MA, et al. Three *Toxoplasma gondii* Dense Granule Proteins Are Required for Induction of Lewis Rat Macrophage Pyroptosis. Bruckner Lodoen M, editor. *mBio*. 2019; 10: e02388–18. <https://doi.org/10.1128/mBio.02388-18> PMID: [30622189](https://pubmed.ncbi.nlm.nih.gov/30622189/)
126. Liue J, enedikt Muller UB, Steinfeldt T, Howard JC. Reciprocal virulence and resistance polymorphism in the relationship between *Toxoplasma gondii* and the house mouse. *eLife*. 2013; 2. <https://doi.org/10.7554/eLife.01298> PMID: [24175088](https://pubmed.ncbi.nlm.nih.gov/24175088/)
127. Yamamoto M, Ma JS, Mueller C, Kamiyama N, Saiga H, Kubo E, et al. ATF6 $\beta$  is a host cellular target of the *Toxoplasma gondii* virulence factor ROP18. *The Journal of Experimental Medicine*. 2011; 208: 1533–1546. <https://doi.org/10.1084/jem.20101660> PMID: [21670204](https://pubmed.ncbi.nlm.nih.gov/21670204/)
128. Haldar AK, Foltz C, Finethy R, Piro AS, Feeley EM, Pilla-Moffett DM. Ubiquitin systems mark pathogen-containing vacuoles as targets for host defense by guanylate binding proteins. *Proceedings of the National Academy of Sciences of the United States of America*. 2015; 112. <https://doi.org/10.1073/pnas.1515966112> PMID: [26417105](https://pubmed.ncbi.nlm.nih.gov/26417105/)
129. Blanchard N, Shastri N. Topological journey of parasite-derived antigens for presentation by MHC class I molecules. *Trends in Immunology*. 2010; 31: 414–421. <https://doi.org/10.1016/j.it.2010.08.004> PMID: [20869317](https://pubmed.ncbi.nlm.nih.gov/20869317/)
130. Liu Q, Zhang D, Hu D, Zhou X, Zhou Y. The role of mitochondria in NLRP3 inflammasome activation. *Molecular Immunology*. 2018; 103: 115–124. <https://doi.org/10.1016/j.molimm.2018.09.010> PMID: [30248487](https://pubmed.ncbi.nlm.nih.gov/30248487/)
131. Bruchard M, Rebé C, Derangère V, Togbé D, Ryffel B, Boidot R, et al. The receptor NLRP3 is a transcriptional regulator of TH2 differentiation. *Nature Immunology*. 2015; 16: 859–870. <https://doi.org/10.1038/ni.3202> PMID: [26098997](https://pubmed.ncbi.nlm.nih.gov/26098997/)
132. Zhao Y, Shao F. NLRC5: a NOD-like receptor protein with many faces in immune regulation. *Cell Research*. 2012; 22: 1099–1101. <https://doi.org/10.1038/cr.2012.83> PMID: [22613950](https://pubmed.ncbi.nlm.nih.gov/22613950/)

133. Howe DK, Sibley LD. *Toxoplasma gondii* comprises three clonal lineages: correlation of parasite genotype with human disease. *The Journal of Infectious Diseases*. 1995; 172: 1561–1566. <https://doi.org/10.1093/infdis/172.6.1561> PMID: 7594717
134. Khan A, Jordan C, Muccioli C, Vallochi AL, Rizzo LV, R B Jr, et al. Genetic divergence of *Toxoplasma gondii* strains associated with ocular toxoplasmosis, Brazil. *Emerging Infectious Diseases*. 2006; 12: 942–949.
135. McLeod R, Boyer KM, Lee D, Mui E, Wroblewski K, Karrison T, et al. Prematurity and severity are associated with *Toxoplasma gondii* alleles (NCCCTS, 1981–2009). *Clinical infectious diseases: an official publication of the Infectious Diseases Society of America*. 2012; 54: 1595–1605. <https://doi.org/10.1093/cid/cis258> PMID: 22499837
136. Grigg ME, Ganatra J, Boothroyd JC, Margolis TP. Unusual Abundance of Atypical Strains Associated with Human Ocular Toxoplasmosis. *The Journal of Infectious Diseases*. 2001; 184: 633–639. <https://doi.org/10.1086/322800> PMID: 11474426
137. Gilbert RE, Freeman K, Lago EG, Bahia-Oliveira LMG, Tan HK, Wallon M, et al. Ocular Sequelae of Congenital Toxoplasmosis in Brazil Compared with Europe. *PLoS Neglected Tropical Diseases*. 2008; 2: 1–7. <https://doi.org/10.1371/journal.pntd.0000277> PMID: 18698419
138. Boothroyd JC. Expansion of host range as a driving force in the evolution of *Toxoplasma*. *Memorias do Instituto Oswaldo Cruz*. 2009; 104: 179–184. <https://doi.org/10.1590/s0074-02762009000200009> PMID: 19430641
139. Tobin CM, Knoll LJ. A Patatin-Like Protein Protects *Toxoplasma gondii* from Degradation in a Nitric Oxide-Dependent Manner. *Infect Immun*. 2012; 80: 55. <https://doi.org/10.1128/IAI.05543-11> PMID: 22006568
140. Donald RGK, Roos DS. Gene knock-outs and allelic replacements in *Toxoplasma gondii*: HXGPRT as a selectable marker for hit-and-run mutagenesis. *Molecular and Biochemical Parasitology*. 1998; 91: 295–305. [https://doi.org/10.1016/s0166-6851\(97\)00210-7](https://doi.org/10.1016/s0166-6851(97)00210-7) PMID: 9566522
141. Huynh MH, Carruthers VB. Tagging of endogenous genes in a *Toxoplasma gondii* strain lacking Ku80. *Eukaryotic Cell*. 2009; 8: 530–539. <https://doi.org/10.1128/EC.00358-08> PMID: 19218426
142. Kim S-K, Karasov A, Boothroyd JC. Bradyzoite-Specific Surface Antigen SRS9 Plays a Role in Maintaining *Toxoplasma gondii* Persistence in the Brain and in Host Control of Parasite Replication in the Intestine. *Infect Immun*. 2007; 75: 1626. <https://doi.org/10.1128/IAI.01862-06> PMID: 17261600
143. Panas MW, Ferrel A, Naor A, Tenborg E, Lorenzi HA, Boothroyd JC. Translocation of Dense Granule Effectors across the Parasitophorous Vacuole Membrane in *Toxoplasma*-Infected Cells Requires the Activity of ROP17, a Rhoptry Protein Kinase. Sullivan WJ, editor. *mSphere*. 2019; 4. <https://doi.org/10.1128/mSphere.00276-19> PMID: 31366709
144. Camejo A, Gold DA, Lu D, McFetridge K, Julien L, Yang N, et al. Identification of three novel *Toxoplasma gondii* rhoptry proteins. *International Journal for Parasitology*. 2014; 44: 147–160. <https://doi.org/10.1016/j.ijpara.2013.08.002> PMID: 24070999
145. Heaslip AT, Nishi M, Stein B, Hu K. The Motility of a Human Parasite, *Toxoplasma gondii*, Is Regulated by a Novel Lysine Methyltransferase. *PLoS Pathogens*. 2011; 7: 1–21. <https://doi.org/10.1371/journal.ppat.1002201> PMID: 21909263
146. Rauch I, Deets KA, Ji DX, von Moltke J, Tenthoery JL, Lee AY, et al. NAIP-NLRC4 Inflammasomes Coordinate Intestinal Epithelial Cell Expulsion with Eicosanoid and IL-18 Release via Activation of Caspase-1 and -8. *Immunity*. 2017; 46: 649–659. <https://doi.org/10.1016/j.immuni.2017.03.016> PMID: 28410991
147. Minot S, Melo MB, Li F, Lu D, Niedelman W, Levine SS, et al. Admixture and recombination among *Toxoplasma gondii* lineages explain global genome diversity. *Proceedings of the National Academy of Sciences of the United States of America*. 2012; 109: 13458–13463. <https://doi.org/10.1073/pnas.1117047109> PMID: 22847430